C.P. No. 625

C.P. No. 625

MINISTRY OF AVIATION

AERONAUTICAL RESEARCH COUNCIL

CURRENT PAPERS

Notes on some Experimental and Theoretical Results for the Boundary Layer Development aft of the Shock in a Shock-Tube

By

L. Bernstein

LONDON: HER MAJESTY'S STATIONERY OFFICE

1963

SIX SHILLINGS NET

C.P. No.625

Notes on some Experimental and Theoretical Results for the Boundary Layer Development aft of the Shock in a Shock-Tube*

- By -
L. Bernstein

Communicated by Professor A. D. Young

April, 1961

SUMMARY

A review of the theoretical work of previous authors is given, and their assumptions and results are discussed in relation to the available experimental evidence. A method of calculating the development of the boundary layer, laminar and turbulent, is then presented in which the usual assumption of small disturbances due to boundary-layer growth is not made and account is taken of the equation of mass continuity in the tube; the resulting momentum equation is integrated numerically.

It is shown that a longitudinal pressure gradient is induced, and that the flow behind the shock-wave accelerates as a result of the constrictive effect of the boundary layer, these effects being more marked for a turbulent boundary layer than for a laminar boundary layer.

Contents

---

1. Introduction/

---

*This work was carried out at Queen Mary College, University of London, and has been submitted as part of a thesis for the degree of Ph.D.

Replaces A.R.C.22,753.

1. Introduction

The shock-tube and its several modifications have now become an accepted tool in gas-dynamic research. However, many aspects relating to its performance, still remain to be adequately explained. In particular, viscous forces within the flowing gases considerably reduce the expected performance, and their action is imperfectly understood.

The condition of no slip between a wall and the gas adjacent to it leads to a momentum defect in the gas flowing close to the wall, which is balanced by a shear force acting on the wall. The boundary layer in which this momentum defect takes place, considerably modifies the flow in a shock-tube, and one result is that the shock-wave does not travel at constant velocity. Furthermore, the gas between the shock-wave and the cold front, or interface (which separates the driver gas from that initially in the channel), is no longer uniform as a result of the perturbations introduced by the growing boundary layers, and it is this gas which is usually used as the test sample.

The channel gas is first set into motion by the arrival of the shock-wave, and we may expect the boundary layer to develop immediately behind this shock. Similarly in the chamber gas, the boundary layer will begin downstream of the leading edge of the rarefaction wave, and these boundary layers will extend throughout the regions of flowing gas, Fig.1.

In the present case, of course, where the flow temperature differs considerably from that of the wall, a thermal boundary layer will also be present, and heat will be transferred perpendicular to the wall. This heat transfer and the work done by the shearing stresses lead to an energy interchange between the flow as a whole and the walls of the shock-tube, and as a result of this interaction we may expect disturbances to be generated in the flow which ultimately overtake the shock-wave and alter its strength.

It is clear that the development of the boundary layers in the unsteady, imperfect gas flow in the shock-tube is highly complex, and in order that any solution may be obtained simplifying assumptions are necessary. Those made by previous investigators are reviewed in the following section, and subsequently by removing some of these restrictive assumptions, an analysis is developed which accounts for some of the observed effects in the shock-tube. However, in this analysis attention is confined to the hot flow between the shock-wave and the interface, and consequently no attempt has been made to extend the analysis to a prediction of shock-wave attenuation. As discussed in Section 2, an analysis based only on this portion of the flow leads to erroneous conclusions regarding the effects of the driver gas, and consequently its use in predicting shock-wave attenuation cannot be justified. Thus, while it is felt that the present analysis is an advance on previous ones, it by no means resolves all the points of conflict between theory and experiment.

2. Review of Previous Work

A number of investigators have examined the attenuation of shock-waves in the shock-tube, both from an experimental and a theoretical standpoint. Among the more important experimental investigations are those of Jones (1957),* Trimpi and Cohen (1955),

Emrich/

---

*An alphabetical list of references is appended.

Emrich and Curtis (1953), Emrich and Wheeler (1958) and Wittliff and Wilson (1957). Theoretical approaches have been made by Trimpi and Cohen (loc. cit.), Mirels (1956), Hollyer (1956), Mirels and Braun (1957) and Spence and Woods (1959).

Of the experimental results, only Jones and Wittliff and Wilson have measured the trajectories for strong shocks, while Emrich and Wheeler, in addition to attempting to correlate measurements of the attenuation of weak shocks in a variety of tubes by a large number of investigators, also present measurements of the density and pressure variations with time at fixed stations along the tube.

Jones and Wittliff and Wilson investigated the effects of different driver gases, hydrogen and helium being employed in both investigations and a combustion driver in the latter. The two sets of results are widely divergent in some respects. The former obtained smooth trajectories (which may have been due solely to the averaging technique used in analysing the results), while those of Wittliff and Wilson exhibit marked fluctuations in the rate of deceleration of the shock-wave when using hydrogen as the driver gas. With the helium driver, the attenuation is considerably reduced for the same initial shock strength - in the experiments of Jones by about half that suffered with the hydrogen driver, while in those of Wittliff and Wilson there was practically no attenuation. This discrepancy is reported as perhaps being due to the fact that, in the latters' experiments, the chamber cross-sectional area was considerably larger than that of the channel. However on these grounds different attenuation rates would be expected in the two tubes with the hydrogen driver, but such differences do not occur.

In none of these experiments on shock-wave attenuation is any significant effect found for changes in the initial channel pressure for constant shock-wave Mach number - that is Reynolds number seems relatively unimportant.

In some experiments by Duff (1959), however, for very low channel pressures - less than 1 mm Hg - significant differences in the shock trajectories do occur with changes of channel pressure. It would seem that in this region of very low channel pressures Reynolds number plays a large part in the flow.

All the theoretical models predict a definite dependence on Reynolds number, this arising since all assume that the shock-wave attenuation is due to the growth of the boundary layers in the flowing gases and for the estimation of this growth they assume the characteristics of the steady flow boundary layers.

Trimpi and Cohen use a one-dimensional, perfect gas theory in which the properties at any lengthwise position in the shock-tube are averaged across the section. The shear stresses and heat transfer are assumed to act at every point in the flowing gases, and to generate one-dimensional disturbances continuously. These disturbances are then assumed to propagate at the local sonic velocity (the values in the ideal gas flow are used) relative to the gas stream, upstream and downstream. Using a small perturbation method they reduce the problem to one involving the integration of the skin-friction along particle paths, that is to the equivalent steady flow problem.

Both the hot gas region behind the shock-wave and the cold region behind the interface are considered, and upstream waves

travelling/

travelling in the hot gas are considered to be partially reflected at the interface, while the disturbances from the cold region are considered to be refracted at this entropy discontinuity. The combination of these disturbances arrives continuously at the shock front, and is shown to reduce its strength.

Among the other assumptions made in their analysis, Trimpi and Cohen take the rarefaction wave to be of zero thickness, a kind of "negative shock", moving with the velocity of sound in the undisturbed chamber gas.

In the numerical evaluation of the theory they assume that the skin-friction dependence on the flow length is identical to that in steady, incompressible flow over a flat plate. For weak shocks the theory predicts attenuation moderately well, but the dependence on Reynolds number is not borne out by experiment.

The use of the steady incompressible flow solution for the skin-friction integral is clearly a very crude approximation, and in particular their solution limits the application to thin boundary layers where an inviscid potential flow exists outside these layers.

Mirels (1956) criticises the theory of Trimpi and Cohen on the grounds that the entropy changes which they postulate as being convected downstream with the ideal flow velocity, would in fact remain in the boundary layer. His analysis is based on similar initial assumptions, but he postulates the generation of disturbances in a different fashion. He argues, quoting the results of van Dyke (1952) for the impulsive motion of an infinite plate in a compressible viscous fluid, that the waves generated by a boundary layer in the external flow are directly dependent on the normal velocity to the wall at the edge of the boundary layer, and are equivalent to those generated by the wall moving normal to itself with this velocity. By linearising the equations of motion with mass source terms included, he thus reduces the problem to one of calculating this normal velocity at the edges of the boundary layers in both the hot and cold gas flows. He then calculates these for a shock and "thin" expansion wave moving over a flat plate, thus limiting the application of the method to cases in which the boundary layers remain thin relative to the hydraulic radius of the tube. Again a Reynolds number dependence is predicted.

In both of these theories, equivalent flat-plate boundary layers are assumed, so that no account is taken of the overall mass continuity equation in the pipe. Because of the momentum defect within the boundary layer, a pressure gradient must be set up along the pipe, which in turn modifies the boundary-layer thickness. This constrictive effect of the boundary layers in the tube will of course also modify the velocity distribution along the pipe. Neither Trimpi and Cohen, nor Mirels make allowance for this, and neither in consequence predicts the acceleration of the interface which is observed in practice. In fact Trimpi and Cohen predict a falling average velocity of the interface as a result of the disturbances generated by the boundary layers.

Neither theory predicts explicitly the effects of different driver gases on the shock-wave attenuation. The numerical calculations in both cases are presented for air on both sides of the diaphragm, and only by carrying out a detailed computation for different gases can the effects be discovered. This is because the ratio of the properties in the two gases on either side of the interface enter not only into

the/

the reflection and transmission coefficients for those waves impinging on the interface, but also into the calculation of the normal velocity component in Mirels' theory, for example.

In this connection it may be remarked that the two theories differ, in general, in the nature of the disturbances: Mirels predicts the generation of upstream and downstream rarefactions in the hot flow, while Trimpi and Cohen predict upstream compressions and in most cases downstream rarefactions, though in some cases, depending on the flow Mach number and the direction of heat flow, downstream compressions may result.

In spite of these divergences, both theories predict the same order of attenuation for weak shock-waves and provide order of magnitude agreement with experiments for weak shocks.

As a result of the disturbances, predictions of the variation of state properties at a given station in the shock-tube are made by Trimpi and Cohen and by Mirels and Braun (1957). Emrich and Wheeler (1958) have carried out a fairly detailed comparison of these predictions with experimental measurements of the pressure and density variations behind weak shocks at several stations along the channel. They conclude that systematic deviations from the predicted values occur, the Trimpi-Cohen theory being fairly accurate for a diaphragm pressure ratio $P_{41} = 2$, and the Mirels-Braun predictions being better for somewhat stronger shocks, $P_{41} = 10$ and 50. Nitrogen was used in both the chamber and the channel, so that these represent very weak shocks.

Only the Trimpi-Cohen theory makes any attempt to predict the variations of state properties in the cold flow, and these predictions are quite inadequate to describe the experimental results, becoming worse as the distance from the diaphragm increases. An interesting feature of the results presented by Emrich and Wheeler, but not commented on by them, is that for $P_{41} = 10$, at which they plot the density variation at three positions along the channel, the theoretical discontinuity at the interface, evident at 18 tube diameters from the diaphragm, is gradually smoothed away, and has completely disappeared at 151 diameters from the diaphragm.

It may also be noted that for the conditions of some of the experiments reported above, the boundary layer grows to fill the tube at 85 diameters downstream of the diaphragm, before the arrival of the cold front.

It is clear that these two theories are inadequate to represent the behaviour of strong shocks, since the assumptions made initially become steadily more unjustifiable as the shock strength increases. The neglect of the flow in the rarefaction wave becomes serious as the extent of this wave increases. The boundary layers are thicker for strong shocks and tend to fill the tube more rapidly. The linearisation of the equations becomes inapplicable as the magnitude of the disturbances increases - this will also occur at large distances from the diaphragm for all shock strengths as evidenced by the results of Emrich and Wheeler.

More recently, Spence and Woods have put forward a theory, (1959), which considers only the hot flow, but is not restricted to perfect gases. They deal only with the turbulent boundary layer, referring to a solution of the laminar case by Demyanov (1957). In principle they solve the problem of the whole of the flow between the shock-wave and the interface allowing for the boundary-layer growth. In this way, unlike the previous theories outlined they take account

of/

of the condition of mass continuity in the pipe as a whole, assuming a thin boundary layer in order to integrate the equations analytically. The equations of motion are also linearised for small perturbations in shock velocity. The turbulent boundary layer is assumed to be equivalent to the steady, turbulent layer on a flat plate, and the assumption is made that the velocity profiles are similar, obeying a power law in transformed co-ordinates. This latter assumption is made on the basis of an analysis by Spence (1960) of some experimental results obtained by Lobb et al (1955) in a compressible turbulent boundary layer in steady flow.

They also propose a mechanism, heat addition by burning at the interface of the hydrogen driver in the hot compressed air, whereby the shock may be initially accelerated above the ideal theoretical strength, a feature present in many experiments.

The only way in which the driver gas enters into the theory is in a boundary condition which is applied to ensure the compatibility of disturbances on either side of the interface, which is assumed to remain ideal. They predict both a strong dependence on Reynolds number and more attenuation with a helium driver than with hydrogen, both of these results being at variance with experimental evidence. Furthermore, in the useful range of shock-tube lengths, about 100 tube diameters, they predict more than 10% attenuation in shock velocity, which implies more than 20% change in pressure behind the shock. It is questionable whether this comes within the range of a small perturbation analysis.*

The theory does however predict acceleration of the interface - according to the linearised theory it would eventually overtake the shock, but this situation is certainly outside the range of the small-disturbance analysis.

All the available theories of shock-wave attenuation are thus inadequate in some respects at predicting more than order of magnitude agreement with the experimental evidence, and in other respects they are even in qualitative disagreement.

Each of the theories outlined depends to a great extent on the calculation of the structure of the boundary layer. The laminar boundary layer is fairly well understood even in compressible flow, so that the skin-friction may be estimated with confidence, but this is by no means true in the turbulent boundary-layer case. The results of the above theories will therefore depend to a large extent on the particular models chosen. The incompressible solution adopted by Trimpi and Cohen for their numerical example is clearly inadequate, but their analysis is not restricted to this model. Mirels chooses a one-seventh power law profile in physical co-ordinates, but takes some account of the thermal boundary layer by introducing the quadratic temperature-velocity relation due to Crocco (see Young, 1953). Spence and Woods employ a power law also for the velocity distribution within the boundary layer, but use a system of transformed co-ordinates on the basis of some steady compressible flat plate results. The transformation used, due to Howarth (see Young, loc. cit.) is

$$Y = \int_o^y \frac{\rho}{\rho_e}\,dy \quad \text{and} \quad \delta_1 = \int_o^\delta \frac{\rho}{\rho_e}\,dy \qquad \ldots(2.1)$$

and the assumption is that

$$\frac{u'}{u'_e}\Big/$$

---

*In this connection Fig.7 of their paper showing the perturbation pressure seems to be inconsistent with their Fig.6 which depicts the shock velocity as a function of distance from the diaphragm. This is probably due to the omission of a zero after the decimal in the ordinate scale of Fig.7.

$$\frac{u'}{u'_e} = \left(\frac{Y}{\delta_1}\right)^{1/n} \quad \text{for } Y \leq \delta_1 \qquad \ldots(2.2)$$

where u' is the velocity relative to the wall, ρ is the gas density, δ is the boundary-layer thickness and the suffix e represents conditions for $y > \delta$.

Martin (1957) has measured the density profiles in the boundary layer, with an interferometer, behind a moving shock-wave for shock-wave Mach numbers of 1.58 and 2.65. Because of the difficulty of defining δ for his experiments, Martin computed the velocity profiles from the measured density distribution and the Crocco relation, and plotted them against y/δ^*, where δ^* is the boundary-layer displacement thickness, defined by

$$\delta^* = -\int_o^\infty \left\{ \frac{\rho u'}{\rho_e u'_e} - 1 \right\} dy. \qquad \ldots(2.3)$$

He infers a collapse to a universal one-fifth power law - i.e., $n = 5$.

However a closer inspection of his data reveals that this collapse is not so definite. In Fig.2, some of his density profiles are replotted using the transformed variables introduced by Spence and Woods. Only those some distance behind the shock-wave are included, well behind the reported transition point, and it can be seen that these profiles cross each other, indicating no hope of complete similarity. The ratio of velocities relative to the wall are also shown in Fig.2, calculated from Crocco's equation (see equation (3.26) following). The differences between the profiles may be explained in two ways. Either the turbulence was not fully developed, - however transition one inch behind the shock was measured both optically and using a thin-film heat transfer gauge - or the pressure gradients present were sufficient to introduce non-similarity effects.

The shortcomings of existing theories have led the author to consider yet another approach to the calculation of the boundary-layer growth in the hot flow region, and its effects on this flow. Both laminar and turbulent boundary layers are considered. The methods are approximate, and are not entirely free of the shortcomings noted in the other methods. Thus, for example, the turbulent boundary-layer analysis involves the use of empirical relations taken over from steady, compressible flow. The method most closely resembles that of Spence and Woods, but does not make use of the small perturbation assumption. Further, the effects of the interface and subsequent cold flow region on the flow in the hot region are ignored.

The procedure adopted involves the integration of the momentum equation. The unsteady equations are transformed to those for steady flow, with a moving wall as a boundary condition, by considering the motion relative to the shock-wave (Mirels, 1956). The form parameter only, that is the ratio of displacement to momentum thickness, is calculated for the case of flow over a flat plate, and this parameter is carried over to the case of flow inside a pipe. The justification for this is that the form parameter is the ratio of two integral quantities, and as such does not change markedly for small changes in velocity profile. The integration has been carried out numerically, with the aid of a digital computer, thus avoiding the necessity of making further assumptions.

3./

3. The Integral Momentum Equation and the Form Parameter for the Case of a Moving Wall

The equations of unsteady motion defining the passage of a shock-wave over a plane wall are first transformed to those for steady flow, by imposing a velocity, equal and opposite to that of the shock-wave, on the system as a whole. The wall then has a velocity, $u_w = -w_1$ and the flow behind the stationary shock-wave a velocity u_e outside the boundary layer, Fig.3(a). The distance along the wall is here measured from the foot of the shock in the direction of boundary-layer growth, and y, v are the distance and velocity normal to the wall. The equations of motion may then be written as

$$\frac{\partial}{\partial x}(\rho u) + \frac{\partial}{\partial y}(\rho v) = 0 \qquad \ldots(3.1)$$

$$\frac{\partial}{\partial x}(\rho u^2) + \frac{\partial}{\partial y}(\rho uv) = -\frac{dp}{dx} + \frac{\partial \tau}{\partial y} \qquad \ldots(3.2)$$

where the symbols have their usual meanings.

Equation (3.2) may be integrated with respect to y to a value $\bar{h}$ outside the boundary layer

$$\int_o^{\bar{h}} \frac{\partial}{\partial x}(p + \rho u^2)\, dy + [\rho uv]_o^{\bar{h}} = -\tau_w$$

or

$$\frac{\partial}{\partial x}\int_o^{\bar{h}} (p + \rho u^2)\, dy + \rho_e u_e v_e = -\tau_w \qquad \ldots(3.3)$$

where suffix e denotes conditions outside the boundary layer.

Integration of equation (3.1) yields

$$\frac{\partial}{\partial x}\int_o^{\bar{h}} \rho u\, dy + \rho_e v_e = 0 \qquad \ldots(3.4)$$

and eliminating v_e from these equations, we have

$$\frac{d}{dx}\int_o^{\bar{h}} (p + \rho u^2)\, dy - u_e \frac{d}{dx}\int_o^{\bar{h}} \rho u\, dy = -\tau_w. \qquad \ldots(3.5)$$

Now

$$\frac{dp}{dx} = -\rho_e u_e \frac{du_e}{dx}$$

so that

$$-\rho_e u_e \frac{du_e}{dx}\bar{h} + \frac{d}{dx}\int_o^{\bar{h}} \rho u (u - u_e)\, dy + \int_o^{\bar{h}} \rho u \frac{du_e}{dx}\, dy = -\tau_w$$

or

$$\frac{du_e}{dx}\int_o^{\bar{h}} (\rho u - \rho_e u_e)\, dy + \frac{d}{dx}\int_o^{\bar{h}} \rho u (u - u_e)\, dy = -\tau_w. \qquad \ldots(3.6)$$

If/

If we define a momentum thickness as

$$\overline{\theta} = \int_0^{\overline{h}} \frac{\rho u}{\rho_e u_e} \left\{ \frac{u}{u_e} - 1 \right\} dy \qquad \ldots(3.7)$$

and a displacement thickness as

$$\overline{\delta^*} = \int_0^{\overline{h}} \left\{ \frac{\rho u}{\rho_e u_e} - 1 \right\} dy \qquad \ldots(3.8)$$

equation (3.6) becomes

$$\rho_e u_e \frac{du_e}{dx} \overline{\delta^*} + \frac{d}{dx} (\rho_e u_e^2 \overline{\theta}) = - \tau_w \qquad \ldots(3.9)$$

which is the usual form except that τ_w has a negative sign, acting in this case in the opposite direction to x. The use of these definitions for $\overline{\theta}$ and $\overline{\delta^*}$ avoids them assuming negative values. If we now define a form parameter $\overline{H}$ as

$$\overline{H} = \overline{\delta^*}/\overline{\theta} \qquad \ldots(3.10)$$

equation (3.9) may be written:

$$\frac{d\overline{\theta}}{dx} + \overline{\theta} \left\{ (\overline{H} + 2) \frac{1}{u_e} \frac{du_e}{dx} + \frac{1}{\rho_e} \frac{d\rho_e}{dx} \right\} = - \frac{\tau_w}{\rho_e u_e^2} . \qquad \ldots(3.11)$$

Apart from the negative sign accompanying the skin-friction term on the right-hand side, equation (3.11) is the usual form of the integral momentum equation (cf., Young, 1953), but here the velocities are not those relative to the wall, as is usual, and $\overline{\theta}$ and $\overline{\delta^*}$ are differently defined.

For later reference we require the relations connecting $\overline{H}$, $\overline{\theta}$, and $\overline{\delta^*}$ with H, θ and δ^* the values employing the usual definitions involving velocities relative to the wall.
Thus:

$$\theta = \int_0^{\overline{h}} \frac{\rho(u_w - u)}{\rho_e(u_w - u_e)} \left\{ 1 - \frac{u_w - u}{u_w - u_e} \right\} dy \qquad \ldots(3.12)$$

$$\delta^* = \int_0^{\overline{h}} \left\{ 1 - \frac{\rho(u_w - u)}{\rho_e(u_w - u_e)} \right\} dy \qquad \ldots(3.13)$$

and

$$H = \frac{\delta^*}{\theta} . \qquad \ldots(3.14)$$

Rewriting equation (3.12)

$$\theta = \int_0^{\overline{h}} \frac{\rho}{\rho_e} \frac{(u_w - u)}{(u_w - u_e)^2} (u - u_e) \, dy$$

$$= \int_0^{\overline{h}} \frac{\rho}{\rho_e} \frac{u_w u_e}{(u_w - u_e)^2} \left(\frac{u}{u_e} - 1 \right) dy - \int_0^{\overline{h}} \frac{\rho}{\rho_e} \frac{u\, u_e}{(u_w - u_e)^2} \left(\frac{u}{u_e} - 1 \right) dy$$

$$= \int_0^{\overline{h}} \frac{\rho}{\rho_e} \frac{u_w u_e}{(u_w - u_e)^2} \left(\frac{u}{u_e} - 1 \right) dy - \frac{u_e^2}{(u_w - u_e)^2} \overline{\theta} . \qquad \ldots(3.15)$$

If/

If we now introduce the transformation given by equation (2.1) justified on physical grounds* in the steady laminar boundary layer and to some extent by Spence (1960) for the turbulent steady boundary layer, namely

$$Y = \int_o^y \frac{\rho}{\rho_e}\, dy \qquad \ldots(3.16)$$

equation (3.15) becomes;

$$\theta = \frac{u_w u_e}{(u_w - u_e)^2}\,\bar{\delta}_i^* - \frac{u_e^2}{(u_w - u_e)^2}\,\bar{\theta}$$

$$= \frac{\dfrac{u_w}{u_e}\,\bar{\delta}_i^* - \bar{\theta}}{\left\{\dfrac{u_w}{u_e} - 1\right\}^2} \qquad \ldots(3.17)$$

where $\bar{\delta}_i^*$ is the displacement thickness for the moving wall case in incompressible flow, viz.,

$$\bar{\delta}_i^* = \int_o^{\bar{h}} \left\{ \frac{u}{u_e} - 1 \right\} dY. \qquad \ldots(3.18)$$

Similarly equation (3.13) may be written

$$\delta^* = -\bar{\delta}^* + \frac{\dfrac{u_w}{u_e}}{\dfrac{u_w}{u_e} - 1}\,\bar{\delta}_i^*. \qquad \ldots(3.19)$$

The form parameter H is then given by

H/

---

*For the case of the steady laminar boundary with zero pressure gradient and $\omega = 1$ the velocity distribution expressed in terms of Y where

$$Y = \int_o^y \frac{\rho}{\rho_e}\, dy, \qquad \ldots(3.16)$$

is independent of Mach number. It is generally argued with some justification that this result will still hold with good approximation when ω is near to unity and the pressure gradients are small. We extend this argument to the shock-tube flow, and note that precisely the same transformation was put forward by Spence as leading to a similar collapse of the velocity profiles when the boundary layer is turbulent.

$$H = \frac{\left\{ -\bar{\delta}^* + \dfrac{\dfrac{u_w}{u_e}}{\dfrac{u_w}{u_e} - 1}\,\bar{\delta}_i^* \right\}\left\{ \dfrac{u_w}{u_w} - 1 \right\}^2}{\dfrac{u_w}{u_e}\,\bar{\delta}_i^* - \bar{\theta}}$$

$$= \frac{\dfrac{u_w}{u_e}\left\{ \dfrac{u_w}{u_e} - 1 \right\}\bar{\delta}_i^* - \left\{ \dfrac{u_w}{u_e} - 1 \right\}^2 \bar{\delta}^*}{\dfrac{u_w}{u_e}\,\bar{\delta}_i^* - \bar{\theta}} . \qquad \ldots(3.20)$$

If the transformation (3.16) is applied to the definition of $\bar{\theta}$ in equation (3.7) we find

$$\bar{\theta} = \bar{\theta}_i . \qquad \ldots(3.21)$$

Equation (3.20) then becomes,

$$H = \frac{\dfrac{u_w}{u_e}\left\{ \dfrac{u_w}{u_e} - 1 \right\}\bar{H}_i - \left(\dfrac{u_w}{u_e} - 1 \right)^2 \bar{H}}{\dfrac{u_w}{u_e}\,\bar{H}_i - 1} . \qquad \ldots(3.22)$$

For incompressible flow $H = H_i$ and $\bar{H} = \bar{H}_i$ so that equation (3.22) becomes

$$\bar{H}_i = \frac{H_i}{\dfrac{u_w}{u_e}\{H_i - 1\} + 1} . \qquad \ldots(3.23)$$

Substitution of equation (3.23) into (3.22) yields;

$$\bar{H} = \frac{\dfrac{u_w}{u_e} H_i - H}{\left\{ \dfrac{u_w}{u_e} - 1 \right\}\left\{ \dfrac{u_w}{u_e} H_i - \dfrac{u_w}{u_e} + 1 \right\}} \qquad \ldots(3.24)$$

It remains to determine H, the form parameter for steady compressible flow with velocities referred to the wall. Applying the transformation (3.16) to equation (3.13), we get

$\delta^*/$

$$\delta^* = \int_o^{\bar{h}} \left\{ \frac{\rho_e}{\rho} - \frac{u_w - u}{u_w - u_e} \right\} dY$$

$$= \int_o^{\bar{h}} \left(\frac{\rho_e}{\rho} - 1 \right) dY + \int_o^{\bar{h}} \left(1 - \frac{u_w - u}{u_w - u_e} \right) dY$$

$$= \int_o^{\bar{h}} \left(\frac{T}{T_e} - 1 \right) dY + \delta_i^* \qquad \ldots(3.25)$$

where it has been assumed that the pressure remains unchanged across the boundary layer, and the equation of state then becomes

$$\rho T = \rho_e T_e = \text{constant.}$$

If for the purpose of evaluating H it is now assumed that the velocity and thermal boundary layers are of equal thickness, that is that the Prandtl number is unity (Pr = 1), we may write following Crocco (cf. Young, 1953, p.412)

$$\frac{\rho_e}{\rho} = \frac{T}{T_e} = \frac{T_w}{T_e} + \left\{ 1 - \frac{T_w}{T_e} + \frac{(u_w - u_e)^2}{2h_e} \right\} \frac{u_w - u}{u_w - u_e} - \frac{(u_w - u)^2}{2h_e} \qquad \ldots(3.26)$$

where T_w is the wall temperature, h_e is the enthalpy of the flow outside the boundary layer, and the velocities are taken relative to the wall. We may note that for a perfect gas,

$$\frac{u_e^2}{2h_e} = \frac{\gamma - 1}{2} M_e^2. \qquad \ldots(3.27)$$

Substitution of equations (3.26 and 3.27) into equation (3.25) gives on simplification,

$$\delta^* = \frac{T_w}{T_e} \delta_i^* + \frac{\gamma - 1}{2} M_e^2 \left\{ \frac{u_w}{u_e} - 1 \right\}^2 \theta_i. \qquad \ldots(3.28)$$

The same procedure leads to

$$\theta = \theta_i$$

so that

$$H = \frac{T_w}{T_e} H_i + \frac{\gamma - 1}{2} M_e^2 \left\{ \frac{u_w}{u_e} - 1 \right\}^2. \qquad \ldots(3.29)$$

Substituting this expression into equation (3.24) we get,

$$\bar{H} = \frac{\left\{ \frac{u_w}{u_e} - \frac{T_w}{T_e} \right\} H_i - \frac{\gamma - 1}{2} M_e^2 \left\{ \frac{u_w}{u_e} - 1 \right\}^2}{\left\{ \frac{u_w}{u_e} - 1 \right\} \left\{ \frac{u_w}{u_e} (H_i - 1) + 1 \right\}} \qquad \ldots(3.30)$$

and H_i, the incompressible flow value of the form parameter for a stationary wall is known from the Blasius solution for the laminar

boundary-layer/

boundary-layer case, and from the power-law profile for the turbulent case.

4. The Equations for Flow Inside a Pipe

If we assume that the boundary layer does not fill the pipe completely, we may write the momentum equation as (Young and Winterbottom, 1942),

$$-2\pi\bar{a}\tau_w = \frac{d}{dx}\int_o^\delta 2\pi(\bar{a}-y)\,\rho u^2 dy - u_e\int_o^\delta \frac{d}{dx}\{2\pi(\bar{a}-y)\,\rho u\}\,dy$$

$$+\frac{d}{dx}\int_o^\delta p2\pi(\bar{a}-y)\,dy - p_e\frac{d}{dx}\int_o^\delta 2\pi(\bar{a}-y)\,dy \qquad \ldots(4.1)$$

where δ is the boundary-layer thickness, $\bar{a}$ the pipe radius, and y is measured from the wall (see Fig.3(c)).

Making the usual boundary-layer assumption that $dp/dy = 0$, we have,

$$\frac{dp}{dx} = -\rho_e u_e \frac{du_e}{dx} \qquad \ldots(4.2)$$

so that equation (4.1) becomes;

$$-\frac{d}{dx}\int_o^\delta 2\pi(\bar{a}-y)\,\rho u\,(u_e-u)\,dy + \frac{du_e}{dx}\int_o^\delta 2\pi(\bar{a}-y)\,(\rho u-\rho_e u_e)\,dy = -2\pi\bar{a}\tau_w$$

or

$$\frac{d}{dx}\int_o^\delta\left(1-\frac{y}{\bar{a}}\right)\rho_e u_e^2\left(\frac{u}{u_e}-1\right)\frac{\rho u}{\rho_e u_e}\,dy + \frac{du_e}{dx}\int_o^\delta\left(1-\frac{y}{\bar{a}}\right)\rho_e u_e\left(\frac{\rho u}{\rho_e u_e}-1\right)dy = -\tau_w$$

which may be written

$$\frac{d}{dx}(\rho_e u_e^2\bar{\theta}) + \rho_e u_e\frac{du_e}{dx}\bar{\delta}^* = -\tau_w \qquad \ldots(4.3)$$

where we define

$$\bar{\theta} = \int_o^\delta \frac{\rho u}{\rho_e u_e}\left(\frac{u}{u_e}-1\right)\left(1-\frac{y}{\bar{a}}\right)dy \qquad \ldots(4.4)$$

and

$$\bar{\delta}^* = \int_o^\delta\left\{\frac{\rho u}{\rho_e u_e}-1\right\}\left\{1-\frac{y}{\bar{a}}\right\}dy. \qquad \ldots(4.5)$$

Writing/

Writing $\bar{H} = \bar{\delta}^*/\bar{\theta}$ as before we have

$$\frac{d\bar{\theta}}{dx} + \bar{\theta}\left\{ (\bar{H} + 2)\frac{1}{u_e}\frac{du_e}{dx} + \frac{1}{\rho_e}\frac{d\rho_e}{dx} \right\} = -\frac{\tau_w}{\rho_e u_e^2} . \qquad \ldots(4.6)$$

The equation of mass continuity in the pipe must also be satisfied. If we denote by suffix 'o' the values of quantities immediately behind the shock-wave, we have,

$$\int_o^{\bar{a}} 2\pi\rho u\,(\bar{a} - y)\,dy = \pi\bar{a}^2 u_{eo}\rho_{eo} = Q, \text{ say.}$$

Now

$$\int_o^{\bar{a}} 2\pi\rho u\,(\bar{a} - y)\,dy = 2\int_o^{\bar{a}} \pi\,(\rho u - \rho_e u_e)\,(\bar{a} - y)\,dy + \rho_e u_e \pi\bar{a}^2$$

$$= 2\pi\rho_e u_e \bar{a}\bar{\delta}^* + \rho_e u_e \pi\bar{a}^2.$$

Therefore

$$\rho_e u_e = \frac{Q}{2\pi\bar{a}\bar{H}\bar{\theta} + \pi\bar{a}^2} = \frac{\rho_{eo} u_{eo}}{1 + 2\bar{H}\bar{\theta}/\bar{a}} . \qquad \ldots(4.7)$$

It is convenient to write all quantities in dimensionless form, denoted by a double dash - ", in terms of their values immediately aft of the shock-wave. Thus:

$$\rho_e'' u_e'' = \frac{1}{1 + 2\bar{H}\bar{\theta}''} \qquad \ldots(4.8)$$

where $\bar{a}$ is taken as the standard length.

The energy equation outside the boundary layer is written non-dimensionally as

$$\frac{p_e''}{\rho_e''} + \frac{\gamma-1}{2} M_{eo}^2 u_e''^2 = 1 + \frac{\gamma-1}{2} M_{eo}^2$$

and if the flow in this region is isentropic

$$p_e'' = \rho_e''^{\gamma}$$

so that dropping the dashes for convenience;

$$\rho_e = \left\{ 1 + \frac{\gamma-1}{2} M_{eo}^2 (1 - u_e^2) \right\}^{\frac{1}{\gamma-1}} \qquad \ldots(4.9)$$

and

$$\rho_e u_e = u_e \left\{ 1 + \frac{\gamma-1}{2} M_{eo}^2 (1 - u_e^2) \right\}^{\frac{1}{\gamma-1}} . \qquad \ldots(4.10)$$

Also

$$M_e^2 = M_{eo}^2 u_e^2 \frac{\rho_e}{p_e}$$

$$= \frac{M_{eo}^2 u_e^2}{\left\{ 1 + \frac{\gamma-1}{2} M_{eo}^2 (1 - u_e^2) \right\}} \qquad \ldots(4.11)$$

and/

and for later reference, the viscosity is assumed to obey the law

$$\mu_e = T_e^{\omega} = \rho_e^{\omega(\gamma-1)} = \left\{ 1 + \frac{\gamma-1}{2} M_{eo}^2 (1 - u_e^2) \right\}^{\omega} . \qquad \ldots(4.12)$$

If now we assume that the value of $\bar{H}$ in the pipe is that given by equation (3.30) for the flat plate, on the grounds that the factor $(1 - y/a)$ occurs inside the integral in both the numerator and the denominator, and is unlikely to have a large effect, we may write the left-hand side of the momentum equation (4.6) in non-dimensional form in the following way.

From equation (4.8)

$$2\bar{H}\bar{\theta} = \frac{1}{\rho_e u_e} - 1 \qquad \ldots(4.8)$$

so that

$$2\bar{\theta}\frac{d\bar{H}}{dx} + 2\bar{H}\frac{d\bar{\theta}}{dx} = -\frac{1}{\rho_e u_e^2}\frac{du_e}{dx} - \frac{1}{\rho_e^2 u_e}\frac{d\rho_e}{dx}$$

$$= -\frac{1}{\rho_e u_e^2}(1 - M_e^2)\frac{du_e}{dx}$$

or

$$\frac{d\bar{\theta}}{dx} = -\left\{ (1 - M_e^2) + (1 - \rho_e u_e)\frac{u_e}{\bar{H}}\frac{d\bar{H}}{du_e} \right\} \frac{1}{2\bar{H}\rho_e u_e^2}\frac{du_e}{dx} . \qquad \ldots(4.13)$$

Substituting for $\bar{\theta}$ and $d\bar{\theta}/dx$ in the left-hand side of equation (4.6) we obtain:

$$\frac{1}{u_e}\frac{du_e}{dx}\left\{ (M_e^2 - 1) + \left(\frac{1}{\rho_e u_e} - 1 \right)\left(\bar{H} + 1 - \frac{u_e}{\bar{H}}\frac{d\bar{H}}{du_e} \right) \right\} \frac{1}{2\bar{H}} = \left[-\frac{\tau_w}{\rho_e u_e^2} \right]^* \qquad \ldots(4.14)$$

and by differentiating equation (3.30) for $\bar{H}$ we obtain

$$\frac{u_e}{\bar{H}}\frac{d\bar{H}}{du_e} = 1 + (\gamma - 1) M_e^2 + \frac{\frac{u_w}{u_e}}{\frac{u_w}{u_e} - 1}\left\{ 1 - \frac{\bar{H}_i}{\bar{H}}\left(1 + \overline{\gamma - 1}\, M_e^2\right) \right\}$$

$$- \frac{\bar{H}_i}{H_i}\left(1 - \frac{(\gamma-1)}{\bar{H}} M_e^2 \right) \qquad \ldots(4.15)$$

where it may be noted that M_e, T_e, and u_e are treated as variables, and the wall temperature T_w has been regarded as constant. This latter assumption has been shown to be theoretically justifiable by Mirels, and experimentally by Martin (1957).

In/

---

*Note that the individual terms on the R.H.S. of this equation are not in non-dimensional form.

In order to complete the solution of the momentum equation we need to evaluate the R.H.S., that is to obtain a value for the skin-friction. This value will of course, depend upon the structure of the boundary layer, and the laminar and turbulent cases are now treated separately.

5. The Laminar Boundary-Layer Case

It will be recalled that the value of the form parameter $\bar{H}$ to be used in the integral momentum equation (4.14) for the flow behind the shock-wave in a pipe, is to be that for compressible, steady flow over a flat plate. This is on the grounds that $\bar{H}$ is unlikely to be very sensitive to the factor $(1 - y/a)$ which appears in the integral quantities $\bar{\delta}^*$ and $\bar{\theta}$ of which it is the ratio. The assumption of steady flow is justified, since relative to the shock the flow is steady. The equations, including a pressure gradient, are

$$\frac{\partial}{\partial x}(\rho u) + \frac{\partial}{\partial y}(\rho v) = 0 \qquad \ldots(5.1)$$

and

$$\rho u \frac{\partial u}{\partial x} + \rho v \frac{\partial u}{\partial y} = -\frac{dp}{dx} + \frac{\partial}{\partial y}\left(\mu \frac{\partial u}{\partial y}\right) \qquad \ldots(5.2)$$

where we have written for the laminar flow case

$$\tau = \mu \frac{\partial u}{\partial y}.$$

The boundary conditions are;

at $y = 0$; $u = u_w$; $v = 0$; and $\mu = \mu_w$

at $y = \delta$; $u = u_e$; $\partial u/\partial y = 0 = \partial^2 u/\partial y^2$; $\mu = \mu_e$.

Using the transformation (3.16) in the form

$$\eta = \frac{1}{\delta_1}\int_0^y \frac{\rho}{\rho_e}\,dy = \frac{Y}{\delta_1} \qquad \ldots(5.3)$$

where

$$\delta_1(x) = \int_0^\delta \frac{\rho}{\rho_e}\,dy$$

we may deduce from equation (5.2) assuming $\rho\mu = \rho_e\mu_e$ that

$$\rho_w u_w \left[\frac{\partial u}{\partial x}\right]_w - \rho_e u_e \frac{\partial u_e}{\partial x} = \frac{\mu_e \rho_w}{\rho_e \delta_1^2}\left[\frac{\partial^2 u}{\partial \eta^2}\right]_w \qquad \ldots(5.4)$$

since $dp/dx = -\rho_e u_e \dfrac{du_e}{dx}$ from Bernoulli's equation and

$$\mu \frac{\partial u}{\partial y} = \frac{\partial u}{\partial \eta}\frac{\rho\mu}{\rho_e \delta_1} = \frac{\partial u}{\partial \eta}\frac{\mu_e}{\delta_1}.$$

Hence/

Hence

$$\frac{\partial}{\partial y}\left(\mu \frac{\partial u}{\partial y}\right) = \frac{\partial^2 u}{\partial \eta^2} \frac{1}{\delta_1^2} \frac{\rho \mu_e}{\rho_e} .$$

Since the velocity at the wall is constant at u_w,

$$\left[\frac{\partial u}{\partial x}\right]_w = 0$$

so that equation (5.4) becomes

$$-\rho_e u_e \frac{\partial u_e}{\partial x} = \frac{\mu_e^2}{\mu_w} \frac{1}{\delta_1^2} \left[\frac{\partial^2 u}{\partial \eta^2}\right]_w . \qquad \ldots(5.5)$$

It is now assumed that a sufficiently good approximation to the velocity distribution within the boundary layer is given by a Polhausen quartic in the transformed variable η. Thus

$$\frac{u}{u_e} = \sum_{i=0}^{4} a_i \eta^i \qquad \ldots(5.6)$$

for $0 \leqslant \eta \leqslant 1$

with the boundary conditions,

$$u = u_w;\ \mu = \mu_w;\ \rho = \rho_w \text{ at } \eta = 0$$

$$\frac{\partial u}{\partial \eta} = 0 = \frac{\partial^2 u}{\partial \eta^2};\ u = u_e;\ \text{etc., at } \eta = 1.$$

Differentiating equation (5.6)

$$\frac{1}{u_e} \frac{\partial u}{\partial \eta} = \sum_{1}^{4} i a_i \eta^{i-1}$$

and

$$\frac{1}{u_e} \frac{\partial^2 u}{\partial \eta^2} = \sum_{2}^{4} i(i-1)\, a_i \eta^{i-2} .$$

Inserting the boundary conditions;

$$\text{at } \eta = 0;\ u_w = u_e a_o$$

$$\text{at } \eta = 1;\ \frac{u_e}{u_e} = 1 = \sum_{o}^{4} a_i \qquad \ldots(5.7)$$

$$\frac{1}{u_e} \frac{\partial u}{\partial \eta} = 0 = \sum_{1}^{4} i a_i$$

and

$$\frac{1}{u_e} \frac{\partial^2 u}{\partial \eta^2} = 0 = \sum_{2}^{4} i(i-1)\, a_i .$$

Also/

Also at $\eta = 0$, we have using equation (5.5)

$$\left[\frac{\partial^2 u}{\partial \eta^2}\right]_{\eta=0} = u_e 2a_2 = -\frac{\delta_1^2 \mu_w}{\mu_e^2} \rho_e u_e \frac{du_e}{dx}$$

so that

$$a_2 = -\tfrac{1}{2} \delta_1^2 \frac{\mu_w}{\mu_e^2} \rho_e \frac{du_e}{dx} \qquad \ldots(5.8)$$

$$= -\tfrac{1}{2} \Lambda$$

where Λ is defined by equation (5.8).

The skin-friction at the wall is given by

$$\tau_w = \mu_w \left(\frac{\partial u}{\partial y}\right)_w = \frac{\mu_w}{\delta_1} \frac{\rho_w}{\rho_e} \left(\frac{\partial u}{\partial \eta}\right)_w$$

$$= \frac{\mu_e}{\delta_1} a_1 u_e$$

and the solution of equations (5.7 & 8) yields,

$$a_1 = \Lambda/6 + 2\left(1 - \frac{u_w}{u_e}\right)$$

so that

$$\tau_w = \frac{\mu_e u_e}{6\delta_1} \left\{ \Lambda + 12\left(1 - \frac{u_w}{u_e}\right) \right\}$$

or

$$\frac{\tau_w}{\rho_e u_e^2} = \frac{\mu_e}{\rho_e u_e} \left\{ \Lambda + 12\left(1 - \frac{u_w}{u_e}\right) \right\} \frac{1}{6\delta_1} \qquad \ldots(5.9)$$

where it has again been assumed that

$$\rho\mu = \rho_e \mu_e .$$

The R.H.S. of the momentum equation (4.14) is therefore, in non-dimensional form,

$$-\frac{\tau_w}{\rho_e u_e^2} = -\frac{\mu_e}{\rho_e u_e} \frac{1}{6\delta_1} \left\{ \bar{\Lambda} + 12\left(1 - \frac{u_w}{u_e}\right) \right\} R_{eo}^{-1} \qquad \ldots(5.10)$$

where

$$R_{eo} = \frac{\rho_{eo} \bar{a} u_{eo}}{\mu_{eo}}$$

and

$$\bar{\Lambda} = \Lambda R_{eo} .$$

Substituting/

Substituting this value into equation (4.14) and rearranging using the definition of Λ from equation (5.8) we get

$$\frac{1}{u_e}\frac{du_e}{dx}\left\{ (M_e^2 - 1) + \left(\frac{1}{\rho_e u_e} - 1 \right)\left(\overline{H} + 1 + \frac{1}{6}\overline{f}\frac{\mu_w}{\mu_e} - \frac{u_e}{\overline{H}}\frac{d\overline{H}}{du_e} \right) \right\} = \frac{8\overline{H}^2 \mu_e \left(\frac{u_w}{u_e} - 1 \right)}{\overline{f}\, R_{eo} (1 - \rho_e u_e)} \qquad \ldots(5.11)$$

where following Young (1953, p.442) we have written

$$\overline{f} = \delta_1/\overline{\theta}$$

and made use of equation (4.8) so that

$$\delta_1 = \frac{\overline{f}}{2\overline{H}}\left\{ \frac{1}{\rho_e u_e} - 1 \right\}.$$

On the grounds that an evaluation of $\overline{\theta}/\delta_1$ using the Polhausen quartic will not yield a sufficiently accurate value for δ_1, we determine $\overline{f}$ as follows.

From equation (3.17) we have

$$\overline{\theta} = \frac{u_w}{u_e}\overline{\delta}_i^* - \left(\frac{u_w}{u_e} - 1 \right)^2 \theta.$$

Now equation (3.19) may be written for the incompressible flow case;

$$\delta_i^* = \frac{\overline{\delta}_i^*}{\frac{u_w}{u_e} - 1}$$

so that

$$\overline{\theta} = \frac{u_w}{u_e}\left(\frac{u_w}{u_e} - 1 \right)\delta_i^* - \left(\frac{u_w}{u_e} - 1 \right)^2 \theta$$

$$= \theta\left(\frac{u_w}{u_e} - 1 \right)\left\{ \frac{u_w}{u_e} H_i - \frac{u_w}{u_e} + 1 \right\}$$

since

$$\frac{\delta_i^*}{\theta} = \frac{\delta_i^*}{\theta_i} = H_i.$$

Thus

$$\overline{f} = \frac{\delta_1}{\overline{\theta}} = \frac{\delta_1}{\theta\left\{ \frac{u_w}{u_e} - 1 \right\}\left\{ \frac{u_w}{u_e}(H_i - 1) + 1 \right\}}$$

or/

or

$$\bar{f} = \frac{f}{\left\{ \frac{u_w}{u_e} - 1 \right\}\left\{ \frac{u_w}{u_e}(H_i - 1) + 1 \right\}}$$

with $f = \frac{\delta_1}{\theta}$, is the value for the compressible, stationary wall case, given by Young (1953, p.442) as

$$f = 9.072\left\{0.45 + 0.55\frac{T_w}{T_e} + 0.09(\gamma - 1)(Pr)^{\frac{1}{2}} M_e^2 \left(\frac{u_w}{u_e} - 1 \right)^2 \right\}^{1-\omega}$$

the Mach number being taken relative to the wall.

The final expression for $\bar{f}$ is taken therefore as

$$\bar{f} = \frac{9.072\left\{0.45 + 0.55\frac{T_w}{T_e} + 0.09(\gamma - 1)(Pr)^{\frac{1}{2}} M_e^2 \left(\frac{u_w}{u_e} - 1 \right)^2 \right\}^{1-\omega}}{\left(\frac{u_w}{u_e} - 1 \right)\left\{ \frac{u_w}{u_e}(H_i - 1) + 1 \right\}} \qquad \ldots(5.12)$$

Thus with $\bar{f}$ and $\frac{u_e}{\bar{H}}\frac{d\bar{H}}{du_e}$ defined by equations (5.12) and (4.15) respectively, we may write equation (5.11) as

$$x = R_{eo}\int_1^{u_e} \frac{\bar{f}(1 - \rho_e u_e)}{8\bar{H}^2(u_w - u_e)}\left\{\left(\frac{1}{\rho_e u_e} - 1 \right)\left(\bar{H} + 1 + \frac{\bar{f}}{6}\frac{\mu_w}{\mu_e} - \frac{u_e}{\bar{H}}\frac{d\bar{H}}{du_e} \right) + M_e^2 - 1\right\}\frac{du_e}{\mu_e} \qquad \ldots(5.13)$$

with p_e, ρ_e, M_e and μ_e given by equations (4.9 - 12).

It will be recalled that all these quantities are non-dimensional in terms of their respective values immediately aft of the shock-wave, and that the standard length is the tube radius, $\bar{a}$. The strength of the shock is specified by u_w.

We may note also that the Reynolds number R_{eo} immediately aft of the shock-wave may be written in terms of the state of the gas in front of it. That is

$$R_{eo} = \frac{\rho_{eo} u_{eo} \bar{a}}{\mu_{eo}} = \frac{\rho_1 w_1 \bar{a}}{\mu_1}\frac{\mu_1}{\mu_{eo}}$$

$$= W_{11} R T_{12}^{\omega} \qquad \ldots(5.14a)$$

where/

where W_{11} is the shock-wave Mach number,

$T_{12} = T_1 / T_2$ is the shock temperature ratio,

and $R_1 = \dfrac{a_1 \bar{a} \rho_1}{\mu_1}$, a_1 being the sound velocity in region 1, in front of the shock.

For a perfect gas, with $\gamma = 7/5$, we have,

$$M_{eo}^2 = \frac{5 + W_{11}^2}{7W_{11}^2 - 1},$$

$$T_{12} = \frac{36W_{11}^2}{(7W_{11}^2 - 1)(W_{11}^2 + 5)}, \qquad \ldots(5.14b)$$

$$u_w = \frac{6W_{11}^2}{W_{11}^2 + 5}.$$

On the assumption that the wall temperature remains constant, and equal to that of the undisturbed gas in front of the shock, $T_w = T_1$, equation (5.13) has been integrated numerically, for several values of the shock-wave Mach number. The specific heat ratio has been assumed constant at $\gamma = 7/5$ and the index of viscosity dependence on temperature ω, was taken at 0.76. The Prandtl number Pr, was also assumed constant in equation (5.12) at 0.725. The form parameter, H_i in incompressible, steady flow with a stationary wall, was taken as the Blasius value, 2.59.

An estimate of the boundary layer growth was also made as follows;

$$\delta = \int_o^{\delta_1} \frac{\rho_e}{\rho} dY = \int_o^{\delta_1} \frac{T}{T_e} dY$$

and using the Crocco relation, equation (3.26)

$$\delta = \int_o^{\delta_1} \left\{ \frac{T_w(u-u_e)}{T_e(u_w-u_e)} + \frac{u_w-u}{u_w-u_e} + \frac{\gamma-1}{2} M_e^2 \left(1 - \frac{u}{u_e}\right)\left(\frac{u}{u_e} - \frac{u_w}{u_e}\right) \right\} dY$$

$$= \bar{\theta} \left\{ \bar{f} - \frac{\gamma-1}{2} M_e^2 + \bar{H}_i \left[\frac{\frac{T_w}{T_e} - 1}{\frac{u_w}{u_e} - 1} + \frac{\gamma-1}{2} M_e^2 \frac{u_w}{u_e} \right] \right\} \qquad \ldots(5.15)$$

with $$\bar{H}_i = \frac{2.59}{1.59\frac{u_w}{u_e} + 1} \quad \text{from equation (3.23)}$$

and $$\bar{\theta} = \frac{1 - \rho_e u_e}{2 \bar{H} \rho_e u_e}.$$

The/

The results are shown in Figs. 4, plotted against $\frac{x}{\bar{a}} R_1^{-1}$ where R_1 is a Reynolds number based on the sound speed in the undisturbed gas.

For nitrogen $R_1 = 7.18 \times 10^6 \bar{a} \frac{p_1}{760}$ where $\bar{a}$ is the tube radius in feet, and p_1 is the undisturbed gas pressure in mm Hg.

6. The Turbulent Boundary-Layer Case.

The turbulent boundary layer in compressible flow is not nearly so well understood as the laminar boundary layer. In incompressible flow, there exists at least sufficient experimental evidence to enable the formulation of empirical relations which may be used to predict with some confidence the behaviour of steady flows in general terms. In compressible flow very little such information exists. Lobb and others (1955) have investigated the compressible, turbulent boundary layer in steady flows, and as pointed out, Spence (1960) has succeeded in transforming the boundary layer coordinate system in such a way that the velocity profiles almost collapse to obey a single power law. The skin-friction is however very dependent upon the velocity profile within the boundary layer, and in flows subjected to large pressure gradients these velocity profiles are unlikely to remain similar. Such flows are likely to develop in the shock-tube, and it has already been noted that in some measurements made by Martin (1957) in the growing boundary layer behind a shock-wave in a shock-tube no such similarity was evident as that found by Spence in the steady flow case.

However it is true to say that the profiles show a closer similarity in terms of the transformed variable Y (equation 3.16), than in terms of y and in order to obtain some estimate of the magnitude of the generated pressure gradients, Spence's assumption of similarity has been employed, the effect of the index in the velocity profile power law being estimated by using two values, n = 5 & 7. The transformation used is the same therefore as that for the laminar boundary-layer case; viz.

$$\eta = \frac{1}{\delta_1} \int_0^y \frac{\rho}{\rho_e} dy = \frac{Y}{\delta_1} \qquad \ldots(6.1)$$

with

$$\delta_1(x) = \int_0^\delta \frac{\rho}{\rho_e} dy .$$

In order to determine the relevant parameters, Spence adopted the following procedure (a slight modification being necessary for the moving wall case). Following Eckert he introduced the concept of the "mean enthalpy" defined by

$$h_m = 0.5(h_w + h_e) + 0.22(h_r - h_e) \qquad \ldots(6.2)$$

where h_r is the recovery enthalpy, and the constants are empirical.

The friction velocity is then defined in terms of the density evaluated at this mean enthalpy, that is

$$v_*^2 = \frac{\tau_w}{\rho_m} \qquad \ldots(6.3)$$

Within/

Within the laminar sub-layer, the shear stress is assumed constant and equal to

$$\tau = \mu \frac{\partial(u_w - u)}{\partial y} = \tau_w \qquad \ldots(6.4)$$

so that

$$u_w - u = \int_0^y \frac{\tau_w}{\mu} dy = \tau_w \int_0^y \frac{dy}{\mu} .$$

Making the usual assumption that $\rho\mu = \rho_e\mu_e = \rho_m\mu_m$ (or $\omega = 1$),

$$u_w - u = \frac{\tau_w}{\mu_e} \int_0^y \frac{\rho}{\rho_e} dy$$

$$= \frac{\tau_w}{\mu_m} \frac{\rho_e}{\rho_m} Y$$

Thus

$$\frac{u_w - u}{v_*} = \frac{v_* Y}{\nu_m} \frac{\rho_e}{\rho_m} . \qquad \ldots(6.5)$$

In the inner region it is therefore assumed that $\frac{v_* Y}{\nu_m} \frac{\rho_e}{\rho_m}$ is the relevant parameter which is to replace $\frac{v_* y}{\nu}$ in the incompressible case.

The velocity profile power law is therefore written

$$\frac{u_w - u}{v_*} = c\left(\frac{Y v_* \rho_e}{\nu_m \rho_m}\right)^{1/n} \qquad \ldots(6.6)$$

which is consistent with

$$\frac{u_w - u}{u_w - u_e} = \eta^{1/n} . \qquad \ldots(6.7)$$

This of course is the key assumption. It has been justified by Spence (loc.cit) for the steady case, but no such justification exists for the present application. Since we are chiefly interested in the qualitative aspect of the quasi-steady region between the shock-wave and the cold front, it would seem a reasonable starting point with the present state of our knowledge. The arbitrariness of this assumption cannot be too strongly emphasised but it may be pointed out, that all the previous analyses have made this or similar assumptions.

Rearranging equations (6.3 & 6) leads to

$$\frac{\tau_w}{\rho_m (u_w - u_e)^2} = c^{-\frac{2n}{n+1}} \left[\frac{\delta_1 (u_w - u_e)}{\nu_m} \frac{\rho_e}{\rho_m}\right]^{-\frac{2}{n+1}} \qquad \ldots(6.8)$$

where u has been replaced by u_e and Y by δ_1, their values at the edge of the boundary layer.

Further/

Further rearrangement yields;

$$\frac{\tau_w}{\rho_e u_e^2} = \left[\frac{\frac{u_w}{u_e} - 1}{c}\right]^{\frac{2n}{n+1}} \left[\frac{\rho_m}{\rho_e}\right]^{\frac{n+3}{n+1}} \left[\frac{\nu_m}{u_e \delta_1}\right]^{\frac{2}{n+1}} . \qquad \ldots(6.9)$$

The momentum thickness is again defined by

$$\bar{\theta} = \int_0^{\delta} \frac{\rho u}{\rho_e u_e} \left(\frac{u}{u_e} - 1\right) dy$$

so that

$$\bar{\theta} = \bar{\theta}_i = \delta_1 \int_0^1 \frac{u}{u_e} \left(\frac{u}{u_e} - 1\right) d\eta ,$$

using equation (6.1) which upon substitution for u from equation (6.7) gives

$$\bar{\theta} = \frac{\delta_1 \left(\frac{u_w}{u_e} - 1\right)\left(\frac{2u_w}{u_e} + n\right)}{(n+1)(n+2)} . \qquad \ldots(6.10)$$

Eliminating δ_1 between equations (6.9 & 10), we get

$$\frac{\tau_w}{\rho_e u_e^2} = \left\{\frac{n + \frac{2u_w}{u_e}}{c^n (n+1)(n+2)} \frac{\mu_m}{\mu_e} \frac{\nu_e}{u_e \bar{\theta}} \frac{1}{R_{eo}}\right\}^{\frac{2}{n+1}} \frac{\rho_m}{\rho_e} \left(\frac{u_w}{u_e} - 1\right)^2 \qquad \ldots(6.11)$$

where each of the parameters involved is written non-dimensionally in terms of their respective values just aft of the shock, the Reynolds number R_{eo} being as before,

$$R_{eo} = \frac{u_{eo} \bar{a}}{\nu_{eo}} = W_{11} R_1 T^{\omega}_{12} \qquad \ldots(6.12)$$

It should be noted that the assumption that $\omega = 1$ is made only where it is felt that it introduces very small errors, as in the determination of form parameters, representing ratios of relevant boundary layer thicknesses, but in general the assumption is not made, although it is always understood that ω is near unity.

Substitution/

Substitution of the R.H.S. of equation (6.11) into the momentum equation (4.14) yields

$$\left[\left(\frac{1}{\rho_e u_e} - 1\right)\left\{\bar{H} + 1 - \frac{u_e}{\bar{H}}\frac{d\bar{H}}{du_e}\right\} - 1 + M_e^2\right]\frac{1}{u_e}\frac{du_e}{dx} = J.2\bar{H}\left\{\frac{2\bar{H}\mu_e}{R_{eo}(1-\rho_e u_e)}\right\}^{\frac{2}{n+1}}$$

where
$$J = \left\{\frac{n + 2\frac{u_w}{u_e}}{c^n(n+1)(n+2)}\frac{\mu_m}{\mu_e}\right\}^{\frac{2}{n+1}}\frac{\rho_m}{\rho_e}\left(\frac{u_w}{u_e} - 1\right)^2 \qquad \ldots(6.13)$$

Thus $\frac{dx}{du_e}$ is again given as a function only of u_e.

Equation (6.13) has been integrated numerically with the aid of a digital computer to yield $x = x(u_e)$ for several shock-wave Mach numbers, and for $n = 5$ and $n = 7$. It will be recalled that $\bar{H}$ and $\frac{d\bar{H}}{du_e}$ are given by equations (3.30) and (3.15) and that for incompressible flow

$$H_i = 1 + \frac{2}{n} \quad \text{for the stationary wall}$$

and
$$\bar{H}_i = \frac{1 + \frac{2}{n}}{1 + \frac{2u_w}{nu_e}} \quad \text{for the moving wall.} \qquad \ldots(6.14)$$

The values of the constant 'c' in the velocity profile law, equation (6.6) were taken from the corresponding incompressible values as follows;

n	5	7
c	6.20	8.74

and a recovery factor of 0.89 was assumed. Consistent with the assumption of perfect gases, the enthalpy equation (6.2) was replaced by one containing temperatures, and again a value $\omega = 0.76$ was used.

The nature of the assumptions made is somewhat arbitrary, since as pointed out earlier, the velocity profile within the boundary layer does not appear to obey the assumed law. For this reason no attempt has been made to refine the solution so as to include the thermodynamic imperfections present in the hot-flow. In practice the dependence of the viscosity on temperature over the effective range covered here is considerably more complex than the simple relation

$$\mu \propto T^{\omega}$$

However such an approximation is useful though perhaps a lower value of ω than that assumed would be more realistic for the stronger shock-waves, when the temperatures involved are higher.

In/

In a similar manner to that used in Section 5, the boundary layer growth has been estimated from

$$\delta = \int_0^{\delta_1} \frac{\rho_e}{\rho} dY = \int_0^{\delta_1} \frac{T}{T_e} dY$$

and the Crocco relation, (3.26) so that,

$$\delta = \bar{\theta} \left\{ \frac{\delta_1}{\bar{\theta}} - \frac{\gamma-1}{2} M_e^2 + \bar{H}_i \left\{ \frac{\frac{T_w}{T_e} - 1}{\frac{u_w}{u_e} - 1} + \frac{\gamma-1}{2} M_e^2 \frac{u_w}{u_e} \right\} \right\} \qquad \ldots(6.15)$$

where $\bar{H}_i$ is given by equation (6.14), and $\bar{\theta}$ as before by equation (4.8). In this case $\bar{\theta}/\delta_1$ is assumed to be given by equation (6.10).

The Crocco relation with $Pr = 1$, in the form (3.26) is somewhat more justified in the turbulent boundary layer case than in the laminar case, since in the former the transport of heat and momentum both take place almost entirely as a result of the same action - turbulent mixing.

The results of the integration are illustrated in Figs. 5 & 6 where $\delta/\bar{a}$, $\bar{\theta}/\bar{a}$ and p_e/p_{eo} are plotted against $\frac{x}{\bar{a}} R_1^{\frac{-2}{n+1}}$ for several values of shock strength and for $n = 5$ & 7.

The parameter $R_1^{\frac{-2}{n+1}}$ masks the differences between the two values of n and the laminar case, so that a comparison of the three is reserved for the next section, where numerical examples are presented.

It will have been noted that for the turbulent boundary layer the expression for $\bar{\theta}/\delta_1$ and its relation to $\tau_w/(\rho_e u_e^2)$ have been taken as the values for zero pressure gradient. No reliable method of including the effect of pressure gradient on these relations for the turbulent boundary layer, even for incompressible flow, is available, although tentative suggestions have been put forward. These are not supported by sufficient experimental evidence to warrant their extrapolation to the compressible flow case.

It may however be interesting to examine the parameter equivalent to that introduced by Buri (Schlichting, 1955) to take account of the pressure gradient. Analagous with the parameter Λ for the laminar boundary layer, we define Γ as

$$\Gamma = \frac{\theta}{u_w - u_e} \frac{\partial (u_w - u_e)}{\partial x} \left\{ \frac{(u_w - u_e)\theta}{\nu_m} \frac{\rho_e}{\rho_m} \right\}^{\frac{2}{n+1}} \qquad \ldots(6.16)$$

which is the definition used by Buri, modified to accommodate the effects of compressibility and the moving wall.

Noting/

Noting that

$$\frac{\theta}{\bar{\theta}} = \frac{n}{\left(\frac{u_w}{u_e} - 1\right)\left(n + \frac{2u_w}{u_e}\right)}$$

and replacing equation (6.8) by

$$\frac{\tau_w}{\rho_m(u_w - u_e)^2} = \frac{c^{\frac{-2n}{n+1}} + \bar{d}\Gamma}{\left\{\frac{(u_w - u_e)\delta_1}{\nu_m}\frac{\rho_e}{\rho_m}\right\}^{\frac{2}{n+1}}} \qquad \ldots(6.17)$$

following Buri, where $\bar{d}$ is an empirical constant, we find that the integral momentum equation (6.13) becomes

$$\left[\left(\frac{1}{\rho_e u_e} - 1\right)\left(\bar{H} + 1 - \frac{u_e}{\bar{H}}\frac{d\bar{H}}{du_e} - \frac{\bar{d}}{1 + \frac{2}{n}\frac{u_w}{u_e}}\frac{\rho_m}{\rho_e}\right) - (1 - M_e^2)\right]$$

$$\times \frac{1}{u_e}\frac{du_e}{dx} = 2\bar{H}.J.\left[\frac{2\bar{H}\mu_e}{R_{eo}(1 - \rho_e u_e)}\right]^{\frac{2}{n+1}} \qquad \ldots(6.18)$$

The extra term involving $\bar{d}$ would appear to be of the same order of magnitude as the other terms in the same bracket if Buri's value of $\bar{d} = -4$ is adopted.

If equation (6.18) is written as

$$x = \int_1^{u_e} G(u_e)\,du_e$$

the effect of the pressure gradient parameter is to increase the value of the integrand, G - that is, for a given value of x, the change in u_e calculated previously will be too large. The likelihood is that we have overestimated the displacement effect of the boundary layer by ignoring the effect of the pressure gradient on the skin-friction. Such an analysis however, has very little experimental backing for the incompressible steady flow case, and can hardly be applied with much confidence to the present quasi-steady, compressible flow.

7. Comparison of the Effects of Laminar and Turbulent Boundary Layers on the Flow behind a Shock-wave inside a Pipe

In the non-dimensional form of Figs. 4 - 6, the variation of for example, the pressure gradient is masked by the Reynolds number parameter appearing in the abscissa. In order to bring out the significance of the present results some particular cases are considered. The effects of shock strength and of undisturbed channel pressure (that is Reynolds number) are presented separately. In particular, cases are examined for shock-wave

Mach/

Mach numbers, $W_{11} = 3$, 4 and 6 for a constant channel pressure of 10 mm Hg; and then for a constant shock-wave Mach number $W_{11} = 3$, the effects of channel pressure are considered by examining the cases $p_1 = 10$, 25 and 100 mm Hg. Such values are fairly typical of shock-tube operation, and the assumption of constant specific heats made in the foregoing analysis is not too seriously in error. In all cases a tube of 1.5 inches hydraulic diameter is assumed.

In measuring quantities in the shock-tube it is usually practical to have instruments fixed at a particular station in the tube, these then measuring the variation of a particular quantity as a function of time. (An exception to this rule is provided by optical studies which provide a spatial field behind the shock-wave.) Accordingly the abscissae involving the distance behind the shock-wave which appear in Figs. 4 - 6 have been converted to time after shock passage on the assumption that the shock velocity remains constant. For the times considered, the shock attenuation is small, and this is justified.

The pressure and gas velocity on the axis are shown in Figs. 7 and 8 for the above conditions. It can be seen that for constant shock strength - defined by W_{11} - the pressure variation for the laminar boundary layer is small, while that for the turbulent case is quite marked. Furthermore, these pressure gradients are stronger as a fraction of the initial jump across the shock the lower the Reynolds number ($R_1 \propto p_1$). It is this quantity, $\frac{1}{p_{eo}} \frac{dp_e}{dt}$, which is effectively plotted in the lower graph of Fig. 7.

For a constant initial channel pressure, p_1, the variation of pressure in the flow after the shock, assuming a turbulent boundary layer, is seen to increase as the shock strength increases. Again the laminar boundary layer has a small effect.

For low values of p_1, that is of R_1, the index n defining the velocity profile within the turbulent boundary layer is of small significance. However at 100 mm Hg, for the two values of n investigated, 5 and 7, the pressure gradients show marked differences some time after shock passage.

Fig. 8 illustrates the effects of the growing boundary layers on the gas velocity in the isentropic core of the flow behind the shock. Again the laminar boundary layer has a small effect, while the turbulent layer leads to a considerable acceleration of the flow. This acceleration increases with increasing shock strength and decreasing channel pressure.

It is emphasised that these results have been obtained by making several simplifying assumptions, which cannot be strictly justified. For example a universal velocity profile law has been assumed for the turbulent boundary layer which does not appear to have any experimental support in the present circumstances. Furthermore the effect of carrying over the form parameter $\bar{H}$, from the flat plate case to that of flow in the pipe, and thereby ignoring the factor $(1 - y/\bar{a})$ in the integral quantities $\bar{\theta}$ and δ_1 is unknown and may be serious when the boundary layer becomes of comparable thickness with the pipe radius. The points at which $\delta = 0.5\bar{a}$ are indicated on some of the curves of Fig. 7. The effect of pressure gradient on the relation for the skin-friction in the turbulent boundary layer has also been neglected for want of a reliable method of including its effect.

However the general results may be expected to apply qualitatively if not quantitatively - that is, that turbulent boundary layer growth is likely to have a more marked effect on the flow behind the shock than is the

laminar/

laminar layer growth. Accordingly if importance is attached to the uniformity of flow in the hot region, transition to turbulence should be delayed as long as possible - for example by ensuring a minimum of roughness on the tube walls.

The differing magnitudes of the pressure gradients generated by the laminar and turbulent boundary layer growth as predicted by these results, suggest that wall pressure measurements might give some indication of the state of the boundary layer. However the inclusion of a pressure gradient parameter similar to that introduced by Buri for the steady, incompressible turbulent boundary layer would reduce the magnitude of the effects calculated, if Buri's value, $\bar{d} = -4$, is adopted. Thus only if large pressure gradients are measured could a turbulent boundary layer be confidently inferred - the converse, that a negligble gradient implies the existence of a laminar boundary layer is not necessarily true.

8. Notation

a	sound speed
$\bar{a}$	hydraulic radius = 2 × area/perimeter
c	defined by equation (6.6)
d	hydraulic diameter
$\bar{d}$	defined by equation (6.17)
f	$= \delta_1/\theta$
$\bar{f}$	$= \delta_1/\bar{\theta}$
H, H_i	form parameters in stationary wall case - suffix i denotes incompressible flow
$\bar{H}$, $\bar{H}_i$	form parameters in moving wall case - suffix i denotes incompressible flow
h	specific enthalpy
J	defined by equation (6.13)
M_j	flow Mach number in region j
n	velocity profile parameter in turbulent boundary layer
Pr	Prandtl number
p	pressure
R	Reynolds number
T	temperature
t	time
u, v	velocities in x-, y- directions respectively
v_*	friction velocity - $\sqrt{\tau_w/\rho_m}$

W_{11} shock-wave Mach number

Y transformed boundary layer coordinate, equation (2.1)

x, y rectilinear coordinates - Fig. 3

γ specific heat ratio

Γ turbulent boundary layer pressure gradient parameter - equation (6.16)

δ boundary layer thickness

δ_i transformed boundary layer thickness - equation (2.1)

δ^*, δ_i^* boundary layer displacement thicknesses in stationary wall case - suffix i denotes incompressible flow

$\bar{\delta}^*, \bar{\delta}_i^*$ boundary layer displacement thicknesses in moving wall case - suffix i denotes incompressible flow

η $= Y/\delta_i$

θ, θ_i boundary layer momentum thickness in stationary wall case - suffix i denotes incompressible flow

$\bar{\theta}, \bar{\theta}_i$ boundary layer momentum thickness in moving wall case - suffix i denotes incompressible flow

Λ laminar boundary layer pressure gradient parameter - equation (5.8)

μ dynamic viscosity

ρ density

τ skin friction

ω index used to define dependence of viscosity on temperature

Suffices

$1, 2, 3, 4, 5$ refers to quantities in regions so labelled in Fig. 1

o refers to conditions immediately aft of shock-wave

w refers to conditions evaluated at wall

e refers to conditions evaluated on tube axis

m refers to values of properties evaluated at mean enthalpy - equation (6.2)

References/

References

No.	Author(s)	Title, etc.
1	R. E. Duff	Shock-tube performance at low initial pressure. Phys.Fl. 1 p.242, 1959.
2	R. J. Emrich and C. W. Curtis	Attenuation in the shock tube. J.App.Phys. 24 p.360, 1953.
3	R. J. Emrich and D. B. Wheeler	Wall effects in shock-tube flow. Phys.Fl. 1 p.14, 1958.
4	R. N. Hollyer	A study of attenuation in the shock tube. J.App.Phys. 27 (3), 1956.
5	J. J. Jones	Experimental investigation of attenuation of strong shock waves in a shock tube with hydrogen and helium as driver gases. NACA TN 4072, July, 1957.
6	R. K. Lobb, E. M. Winkler and J. Persh	Experimental investigation of turbulent boundary layers in hypersonic flow. J.Ae.Sc. 22 (1) 1, 1955.
7	W. A. Martin	An experimental study of the boundary layer behind a moving plane shock. Univ. of Toronto UTIA Rep. No. 47, 1957.
8	H. Mirels	Boundary layer behind a shock or thin expansion wave moving into a stationary fluid. NACA TN 3712, May, 1956.
9	H. Mirels	Attenuation in the shock tube due to unsteady-boundary-layer action. NACA TN 3278, August, 1956.
10	H. Mirels and W. H. Braun	Nonuniformities in shock-tube flow due to unsteady-boundary-layer action. NACA TN 4021, May, 1957.
11	H. Schlichting	Boundary-layer theory. McGraw-Hill, 1955.
12	D. A. Spence	Velocity and enthalpy distribution in the compressible turbulent boundary layer on a flat plate. J.Fl.Mech. 8 (3) 368, 1960.
13	D. A. Spence and B. A. Woods	Boundary layer and combustion effects in shock-tube flows. Paper delivered at Colston Symposium, Bristol, 1959. Published in "Hypersonic Flow", Butterworth (1960).
14	R. L. Trimpi and N. B. Cohen	A theory for predicting the flow of real gases in shock tubes with experimental verification. NACA TN 3375, March, 1955.
15	M. D. Van Dyke	Impulsive motion of an infinite plate in a viscous compressible fluid. J.App.Math.Phys. 3 (5) 343, 1952.

16/

No.	Author(s)	Title, etc.
16	C. E. Wittliff and M. R. Wilson	Shock-tube driver techniques and attenuation measurements. Cornell Aero. Lab. Rep. AD-1052-A-4, 1957.
17	A. D. Young	Modern developments in fluid dynamics. Ed. L. Howarth. Chapter X. Boundary layers. O.U.P., 1953.
18	A. D. Young and N. E. Winterbottom	High-speed flow in smooth cylindrical pipes of circular cross-section. A.R.C. R. & M. 2068, November, 1942.

FIG.1.

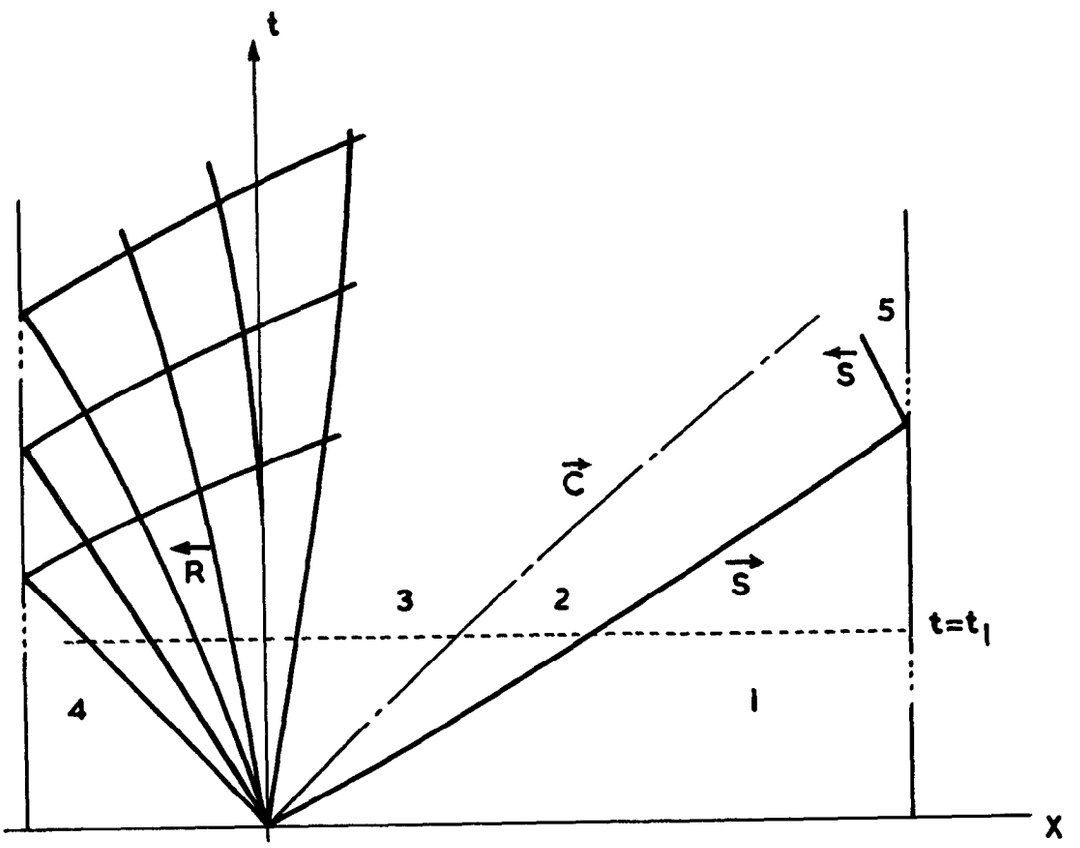

(a)

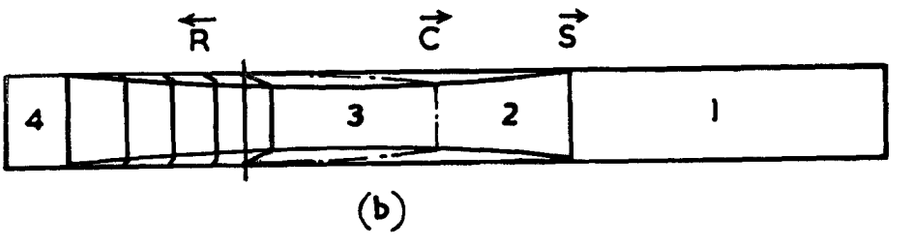

(b)

(a) Distance - time plane.
(b) Physical plane, $t=t_1$

Non - ideal gas flow in the shock - tube.

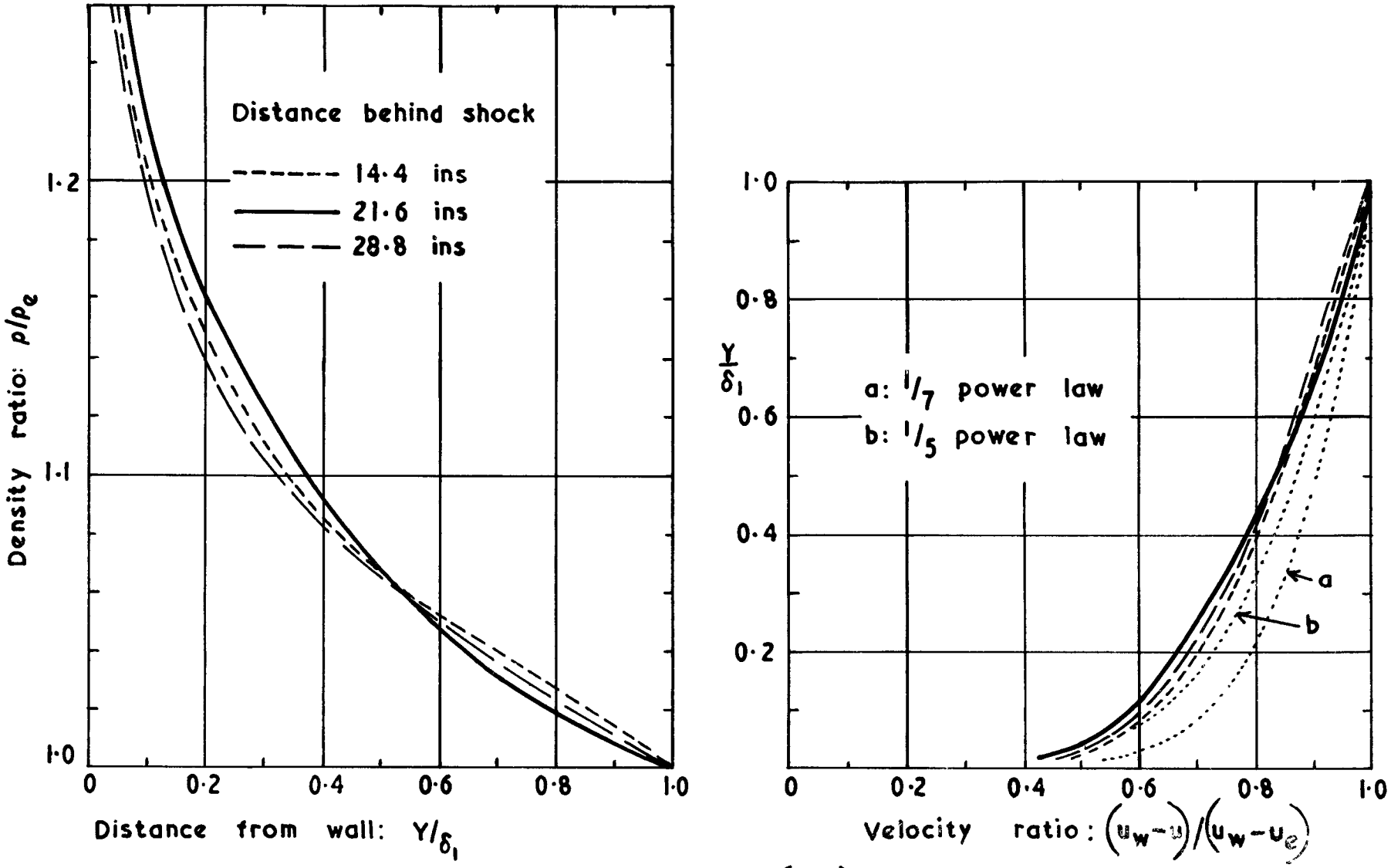

FIG.2.

Boundary layer profiles computed from Martin (1957) $W_{11} = 2{\cdot}65$; $p_1 = 120$ mm Hg.

FIG. 3.

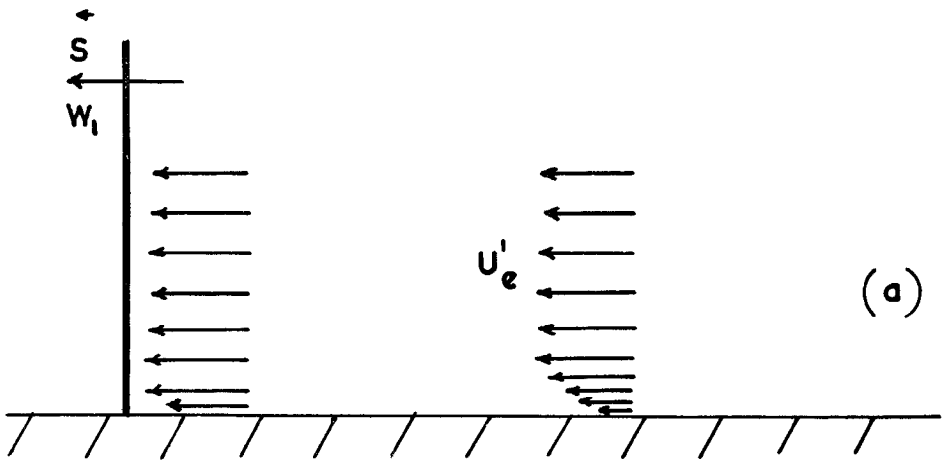

a Flow relative to wall

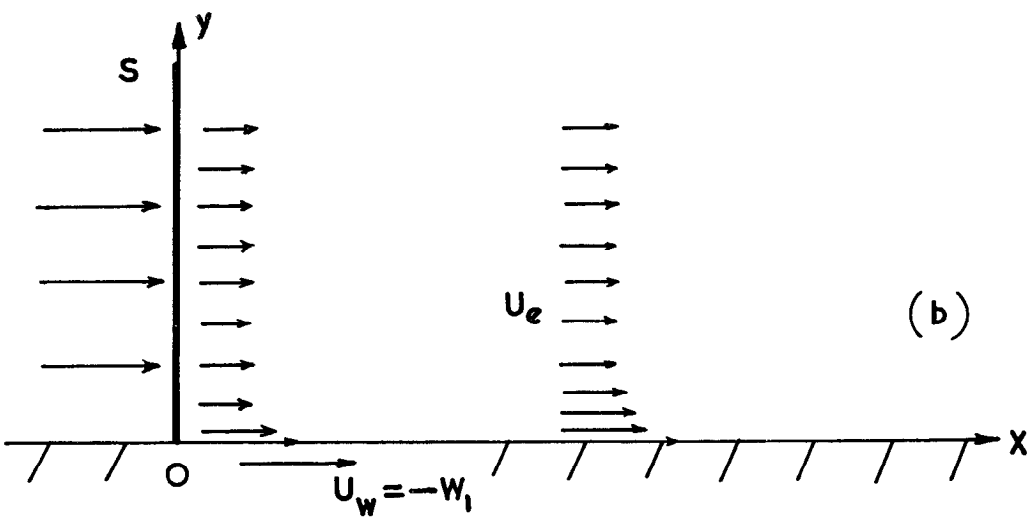

(b)(c) Flow relative to shock—wave

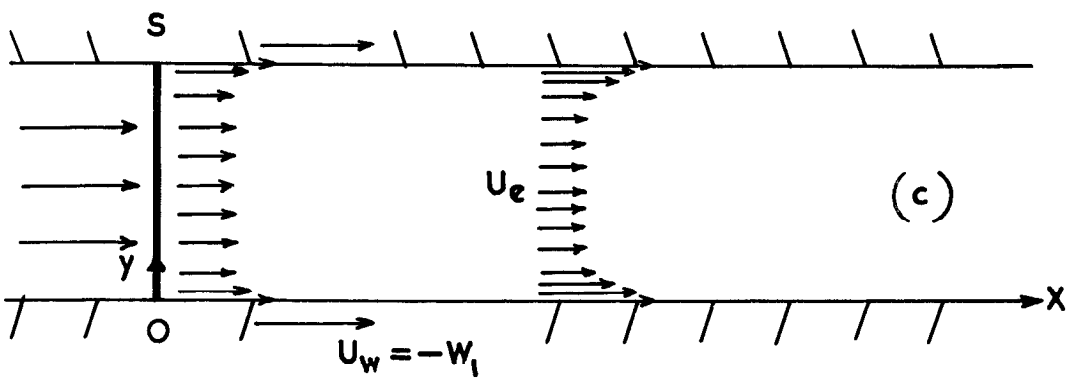

Velocities represented by arrow length, densities by spacing

Coordinate system in transformed flow

FIG. 4.

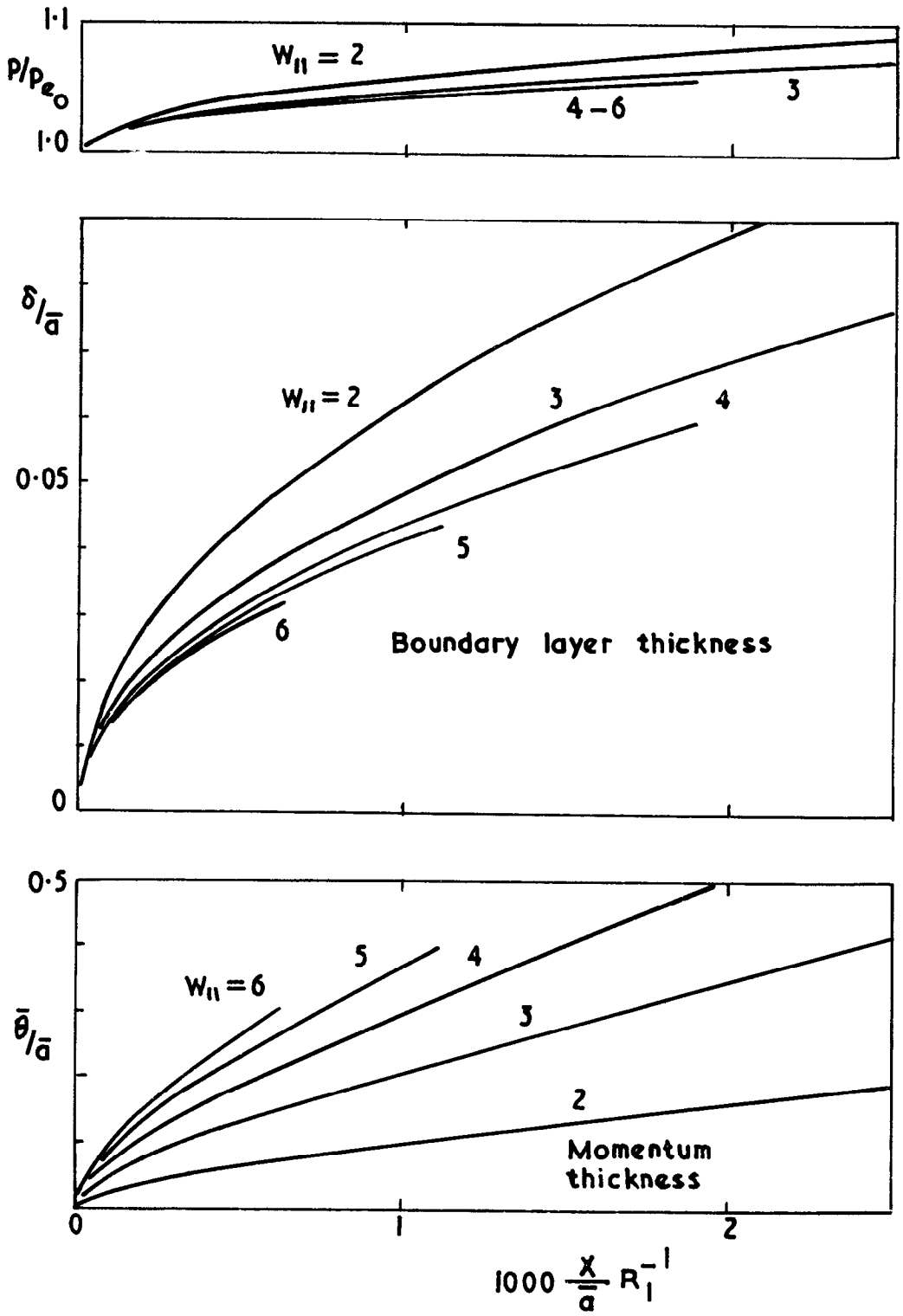

Laminar boundary layer thicknesses and induced pressure rise behind a shock in a pipe.

FIG. 5.

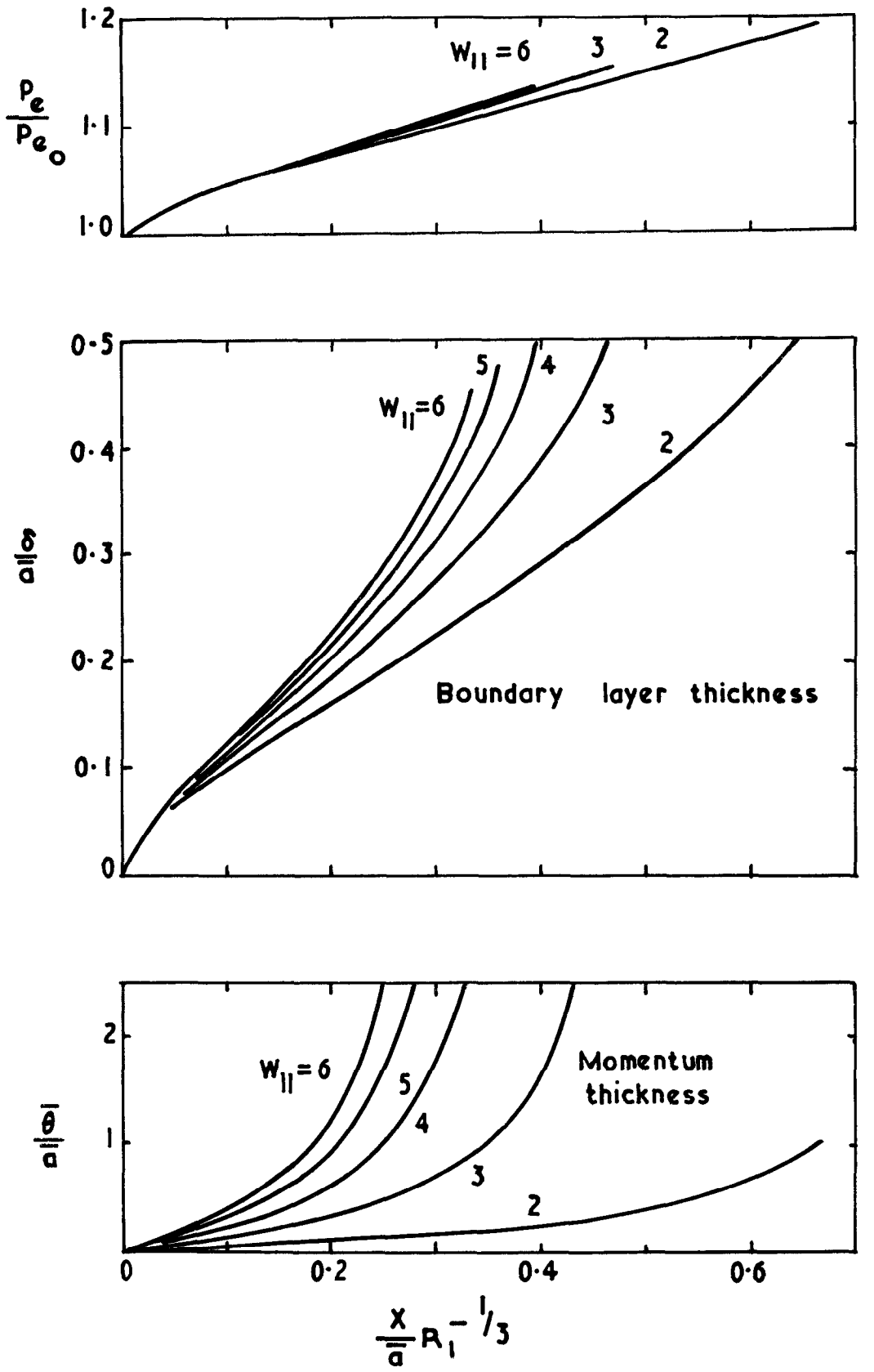

Turbulent (n = 5) boundary layer thicknesses and induced pressure rise behind a shock in a pipe.

FIG. 6.

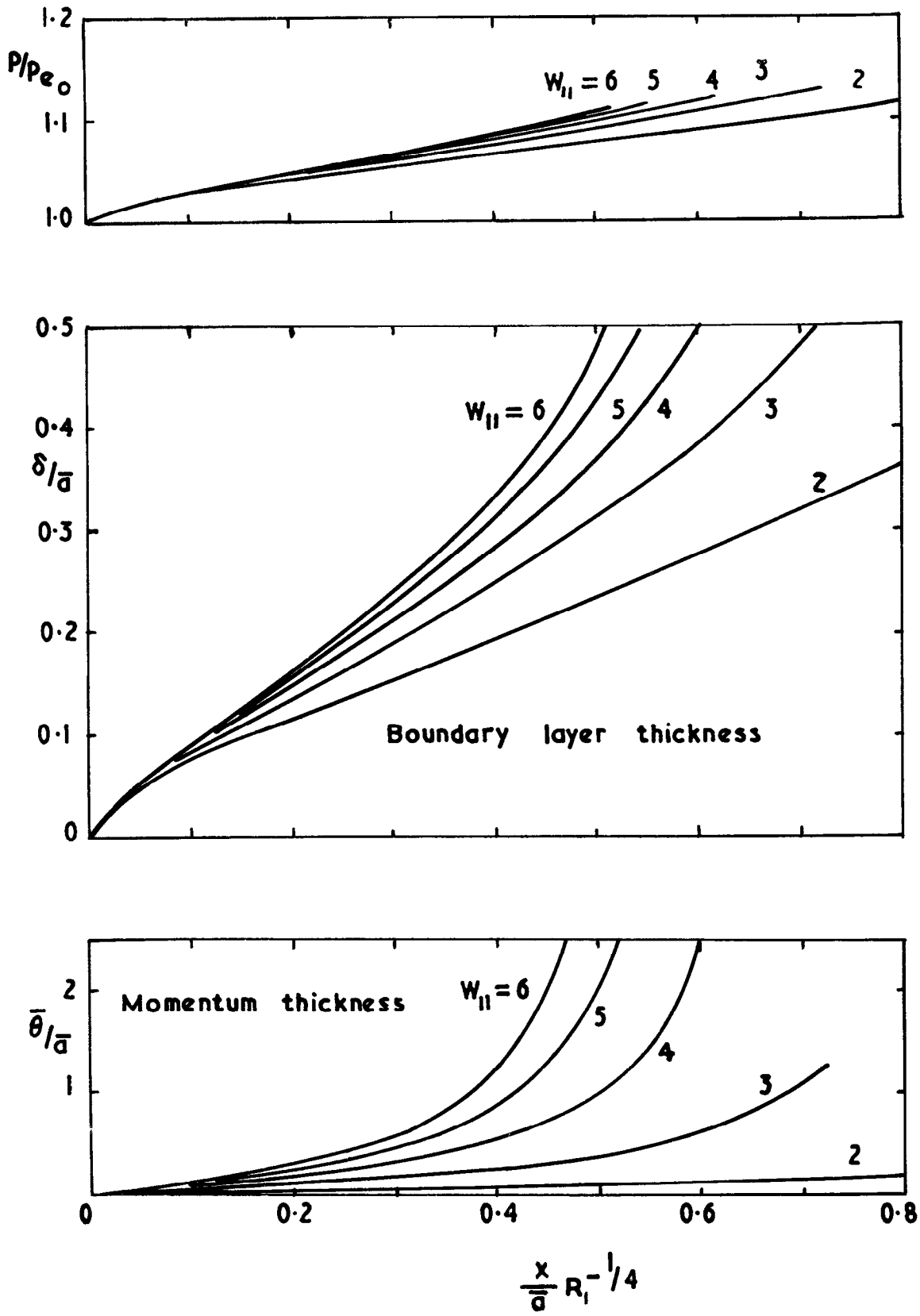

Turbulent (n = 7) boundary layer thicknesses and induced pressure rise behind a shock in a pipe.

FIG. 7.

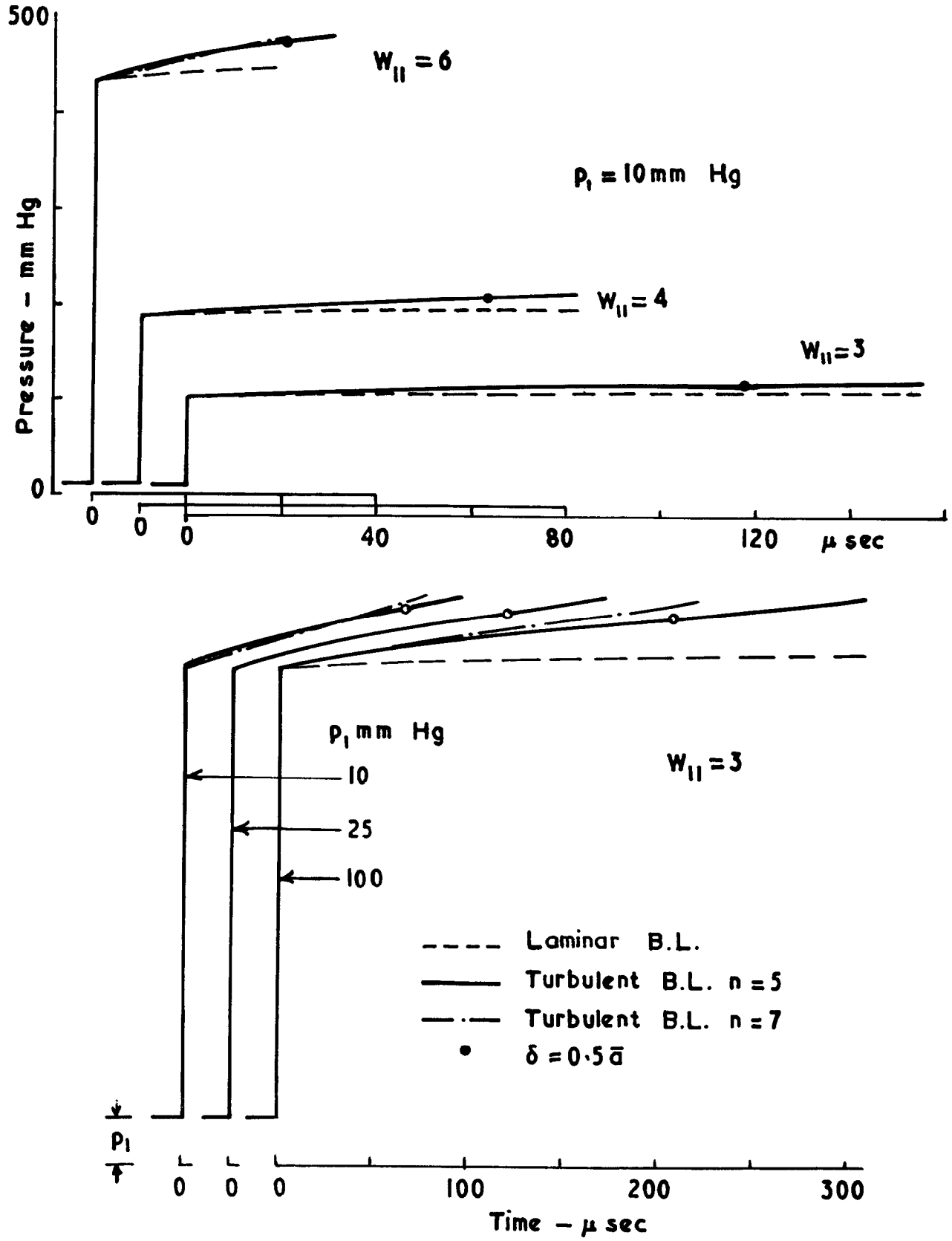

Pressure in 1·5"D tube upon shock passage at Mach No.= W_n

FIG. 8.

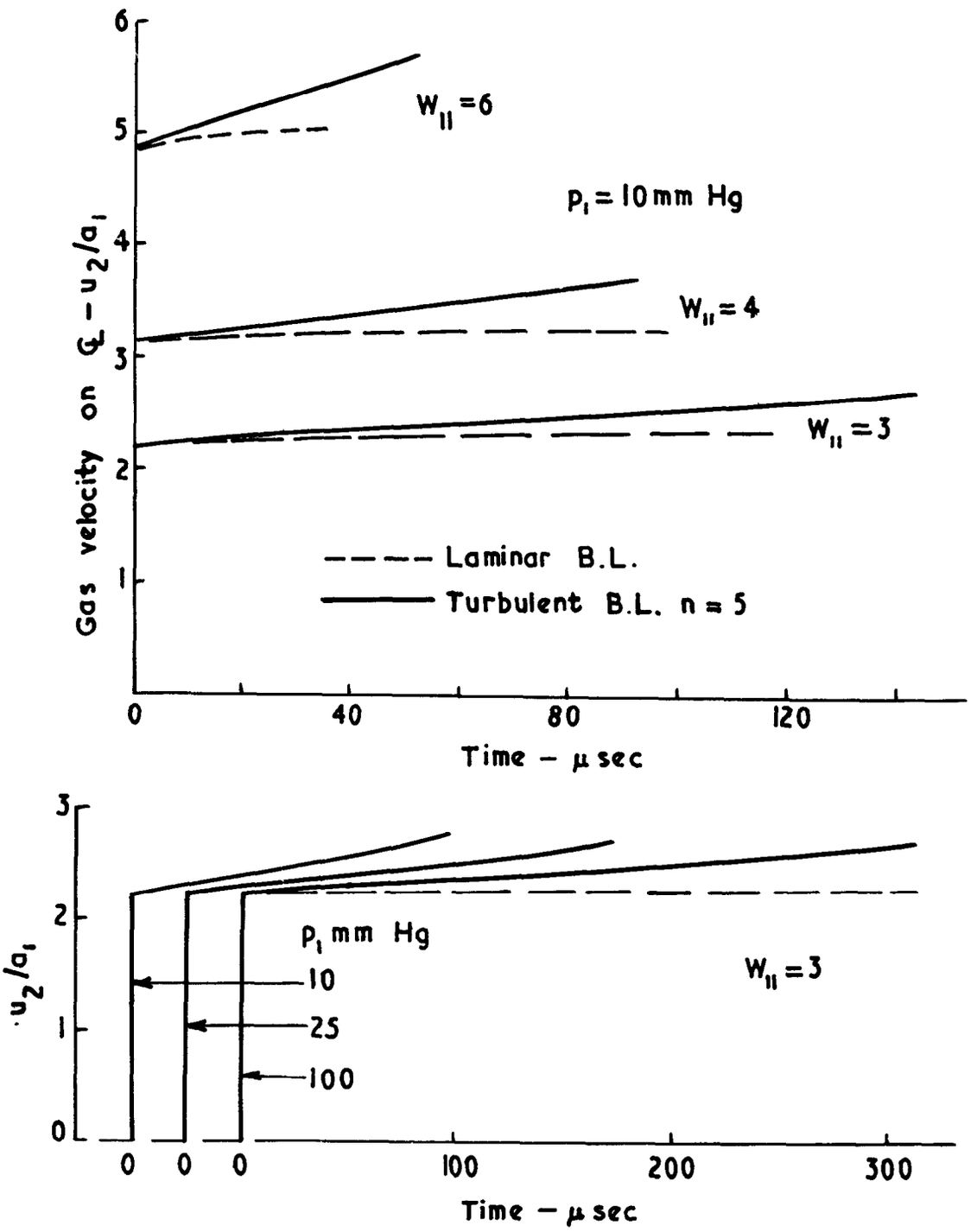

Gas velocity on axis of 1·5" D tube after shock passage at Mach No. = W_{11}.

A.R.C. C.P. No.625
April, 1961
Bernstein, L.

NOTES ON SOME EXPERIMENTAL AND THEORETICAL RESULTS FOR THE BOUNDARY-LAYER DEVELOPMENT AFT OF THE SHOCK IN A SHOCK TUBE

A review of previous work is given, followed by a new approach which takes account of the equation of overall mass continuity in the tube, and does not assume small disturbances.

It is shown that the boundary-layer growth induces a pressure gradient in the flow, and that this flow accelerates. The effects are most marked for a turbulent boundary layer.

A.R.C. C.P. No.625
April, 1961
Bernstein, L.

NOTES ON SOME EXPERIMENTAL AND THEORETICAL RESULTS FOR THE BOUNDARY-LAYER DEVELOPMENT AFT OF THE SHOCK IN A SHOCK TUBE

A review of previous work is given, followed by a new approach which takes account of the equation of overall mass continuity in the tube, and does not assume small disturbances.

It is shown that the boundary-layer growth induces a pressure gradient in the flow, and that this flow accelerates. The effects are most marked for a turbulent boundary layer.

A.R.C. C.P. No.625
April, 1961
Bernstein, L.

NOTES ON SOME EXPERIMENTAL AND THEORETICAL RESULTS FOR THE BOUNDARY-LAYER DEVELOPMENT AFT OF THE SHOCK IN A SHOCK TUBE

A review of previous work is given, followed by a new approach which takes account of the equation of overall mass continuity in the tube, and does not assume small disturbances.

It is shown that the boundary-layer growth induces a pressure gradient in the flow, and that this flow accelerates. The effects are most marked for a turbulent boundary layer.

Printed and published by
HER MAJESTY'S STATIONERY OFFICE

To be purchased from
York House, Kingsway, London w.c.2
423 Oxford Street, London w.1
13A Castle Street, Edinburgh 2
109 St. Mary Street, Cardiff
39 King Street, Manchester 2
50 Fairfax Street, Bristol 1
35 Smallbrook, Ringway, Birmingham 5
80 Chichester Street, Belfast 1
or through any bookseller

Printed in England

S.O. Code No. 23-9013-25